RSC Advances

PAPER

View Article Online
View Journal | View Issue

Cite this: *RSC Adv.*, 2025, **15**, 2930

Ligand-free palladium-catalyzed synthesis of 3-(2,2-dialkyl-2*H*-chromen-4-yl)-2-phenylimidazo[1,2-*a*]pyridine derivatives: molecular docking investigation of their potential as DNA gyrase inhibitors and evaluation of their antibacterial activities†

Rudra Narayan Mishra, [a] Mohammed Ansar Ahemad, [a] Jasmine Panda, [a] Sabita Nayak, *[a] Seetaram Mohapatra [a] and Chita Ranjan Sahoo[b]

Received 30th December 2024
Accepted 9th January 2025

DOI: 10.1039/d4ra09092f

rsc.li/rsc-advances

Palladium-catalyzed reactions between imidazo[1,2-*a*]pyridine derivatives and 4-bromo-2,2-dialkyl-substituted 2*H*-chromenes under microwave irradiation at 100 W, 120 °C for 20–30 min provided a series of new 3-(2,2-dialkyl-2*H*-chromen-4-yl)-2-phenylimidazo[1,2-*a*]pyridine derivatives in good to excellent yields. The structures of the synthesized compounds were confirmed through spectroscopic techniques (NMR and HRMS). The X-ray single-crystal structure of compound **16e** was also determined. Shorter reaction time, high yield and good substrate scope were the major advantages of this method. All these compounds were further investigated *in vitro* for the evaluation of their antibacterial potency using the agar well diffusion method against human pathogenic Gram-negative *E. coli* and Gram-positive *S. aureus* bacteria, with the determination of their minimum inhibitory concentration (MIC) values. Indeed, compound **16h** strongly inhibited DNA gyrase *in silico* with a binding affinity of −8.7 kcal mol^{-1} and exhibited zone of inhibition (ZI) values of 19 mm and MIC values of 10 μg mL^{-1} in both Gram-negative *E. coli* and Gram-positive *S. aureus*, relative to the standard drug gentamicin. By analyzing the structure–activity relationships based on the molecular docking results and the potent antibacterial activities, it could be concluded that these new phenylimidazo[1,2-*a*]pyridine-chromene derivatives have the potential to be effective druggable antibacterial agents.

1. Introduction

In today's world of global health concerns, antimicrobial resistance (AMR) is a serious, comprehensive and multisectoral issue.[1] The global rise in AMR poses a significant threat, as it diminishes the efficacy of common antibiotics against widespread bacterial infections. To combat the issue of antibiotic resistance, a concerted and urgent effort is required to develop new antibiotics with improved toxicity profiles. In this regard, heterocyclic moieties are very important in medicinal chemistry.[2] Hence, this quest has provoked scientists to investigate a wide range of physiologically active heterocycles in order to create effective antibacterial drug candidates.

Among numerous heterocycles, imidazo[1,2-*a*]pyridine (IZP) is the backbone of various marketed drugs, such as alpidem, saripidem, necopidem, zolpidem, olprinone, and zolimidine (Fig. 1).[3–5] IZP is a multitargeted scaffold possessing a wide range of pharmacological activities, such as antibacterial, anticancer, anti-inflammatory, antihypertensive, antiviral, antiosteoporotic, antiparasitic, and neuroprotective properties.[6–10] IZPs can target several enzymes associated with the synthesis of cell wall/peptidoglycan, protein, folic acid, DNA or RNA to eradicate infections. Investigations to date have shown that substituted IZP rings exhibit remarkable antibacterial activity.[11]

IZPs bearing bis-heterocycles show good antibacterial activity, as reported in various literature sources.[11] For instance, Al-Tel *et al.* (2011) reported the synthesis of indole-based-IZPs **5** from **6** and **7** (see Fig. 2a) as antibacterial agents. These compounds exhibited strong inhibition against *S. aureus*, *E. faecalis*, *B. megaterium*, *E. coli*, *P. aeruginosa* and *E. aerogenes*, compared to control antibiotics, such as cefixime and amoxicillin. The nature of the substituents, such as aryl groups, exemplified the extent of the activity of these compounds (Fig. 2a).[12,13] In 2019, Ebenezer

[a]*Organic Synthesis Laboratory, Department of Chemistry, Ravenshaw University, Cuttack 753003, Odisha, India. E-mail: sabitanayak18@gmail.com*

[b]*ICMR-Regional Medical Research Centre, Department of Health Research, Ministry of Health & Family Welfare, Govt. of India, Bhubaneswar 751023, Odisha, India*

† Electronic supplementary information (ESI) available. CCDC 2347891. For ESI and crystallographic data in CIF or other electronic format see DOI: https://doi.org/10.1039/d4ra09092f

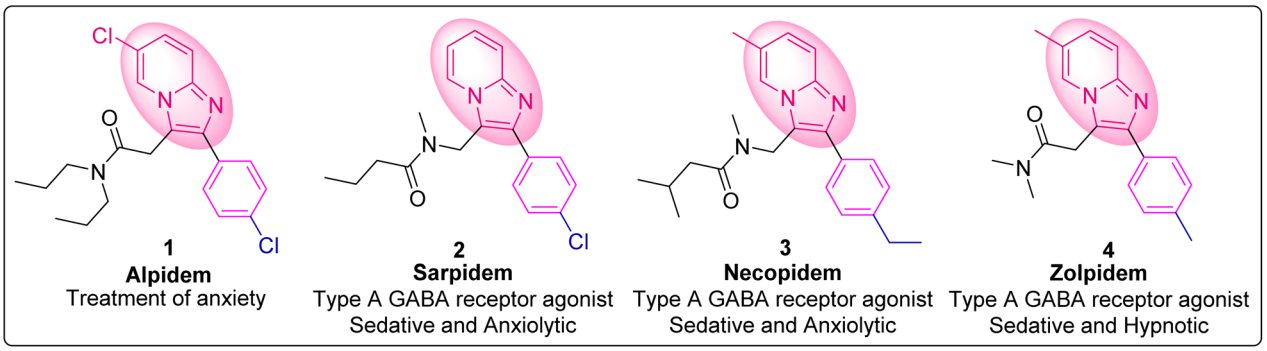

Fig. 1 Clinically used drugs with an imidazo[1,2-*a*]pyridine skeleton.

et al. reported the synthesis of pyrazole-IZP molecular conjugates **8** as antibacterial agents targeting cell wall synthesis from aminopyridine **9**, alkyne **10** and pyrazole aldehyde **11** using $CuSO_4$: sodium ascorbate : Cs_2CO_3 in a ratio of 1 : 2 : 0.2 at 120 °C for 12 h.[14] The compounds displayed pronounced bactericidal activity, as demonstrated by their MIC and time-kill kinetics values (Fig. 2b).[15] Thakur *et al.* (2020) reported the synthesis of IZP-bearing pyran bis-heterocyclic derivatives **12** as potent antibacterial agents from phenylimidazo[1,2-*a*]pyridine-3-carbaldehyde **13**, 5,5-dimethylcyclohexane-1,3-dione **14**, and malononitrile **15** in 5 mL GAAS : 1 mL EtOH at 80 °C. Indeed, antibacterial studies showed significant results for the synthesized compounds against *E. coli*, *S. aureus*, and *S. typhi* (Fig. 2c).[16]

In the quest to develop new antibacterial compounds, our group in 2021 reported 2*H*-chromene-based IZP derivatives as potent peptide deformylase inhibitors from chromene aldehyde and 2-aminopyridine in $FeCl_3$, and $MeNO_2$/DMF under microwave irradiation at 60 W, 100 °C in 15 min. The synthesized compounds exhibited potent antibacterial activity against bacterial strains such as *K. oxytoca*, *S. pyogenes*, *S. aureus*, and *E. coli*.[17] They were synthesized as monosubstituted imidazo[1,2-*a*]pyridine, but we had tried to synthesize disubstituted imidazo[1,2-*a*]pyridine. In our attempts, we tried various different substituents in the phenyl ring of imidazo[1,2-*a*]pyridine moiety and also in the chromene core.

Keeping this idea in mind, in this study we planned to fuse both 4-bromo-2,2-dialkyl-substituted 2*H*-chromenes and the imidazo[1,2-*a*]pyridine moiety in a single molecular entity to construct phenylimidazo[1,2-*a*]pyridine-based chromene hybrid molecules *via* a palladium-catalyzed cross-coupling reaction. To the best of our knowledge, this is the first report on the synthesis and antibacterial activity of 3-(2,2-dialkyl-2*H*-chromen-4-yl)-2-phenylimidazo[1,2-*a*]pyridine derivatives. Molecular docking investigations were further employed to gain better insights into the hybrid's potency while attempting to provide a mechanism for the action of the hybrid compounds as DNA gyrase inhibitors.

2. Results and discussion

2.1 Chemistry

2.1.1. Synthesis. The synthesis of the phenylimidazo[1,2-*a*]pyridine-chromene derivatives was initiated by taking phenylimidazo[1,2-*a*]pyridines **17** and 4-bromo-2,2-dialkyl substituted 2*H*-chromenes **18**. Primarily, phenyl-substituted imidazo[1,2-*a*]pyridines **17(a–d)** were synthesized from 2-chloroacetophenone **20** and 4-Me/5-Me substituted 2-aminopyridine **19** in a solution of H_2O–IPA (1 : 1) under microwave heating at 100 W at 75 °C for 5 min (Scheme 1) following a known literature procedure.[18,19]

After having **17(a–d)** in hand, we further synthesized compounds **18(a–d)**. Initially, *o*-hydroxy acetophenone **21** and substituted ketones **22** reacted by aldol condensation followed by intramolecular cyclization to provide substituted 2*H*-chromones **23**, which then underwent reaction with PBr_3 to give 4-bromo-2,2-dialkyl-substituted 2*H*-chromenes **18(a–d)** (Scheme 2).[20,21]

After the successful synthesis of the starting materials **17a** and **18a**, we further proceeded towards the synthesis of **16a**. Very recently, Raiguru *et al.* from our group[18] reported in 2023 the synthesis of imidazo[1,2-*a*]pyridine-flavone hybrid derivatives using imidazo[1,2-*a*]pyridine and bromo flavone by a Heck coupling reaction using $Pd(OAc)_2$ in 1,4-dioxane and ethanol (2 : 1) at 100 W at 100 °C for 30 min using TPP as a ligand. We applied the same conditions for the coupling of **17a** and **18a**, but unfortunately failed to achieve the coupled product. In order to achieve **16a** by the coupling reaction between **17a** and **18a**, we screened the reaction conditions by trying various palladium catalysts, bases, ligands, and solvents.

The reaction was carried out under both conventional heating as well as microwave irradiation. From Table 1, it can be seen that the optimal reaction conditions were $Pd(OAc)_2$, K_2CO_3 in DMF at 100 W at 120 °C for 20 min, which provided the product **16a** in an 88% yield (Table 1, entry 10). The results obtained from both the conventional and microwave irradiation methods are summarized in Table 1. The product **16a** was characterized by ^1H, ^{13}C NMR, and HRMS analyses.

2.1.2. Elucidation of the structure. The structure of the product **16a** was characterized by ^1H, ^{13}C NMR, and HRMS analyses. The ^1H NMR analysis of imidazo[1,2-*a*]pyridine **17a** displayed a sharp singlet at δ 7.86 ppm, attributed to the C3–H proton, which disappeared in the coupled product **16a**. The ^{13}C NMR analysis of **17a** showed a C–H peak at δ 108.1 ppm, which was shifted to δ 123.7 ppm in product **16a**, appearing as a quaternary carbon. In compound **18a**, **H11** and **H12** appeared as a 6-proton singlet at 1.45 ppm and **C11** and **C12** appeared at 27.5 ppm, while in product **16a**, they appeared at different ppm

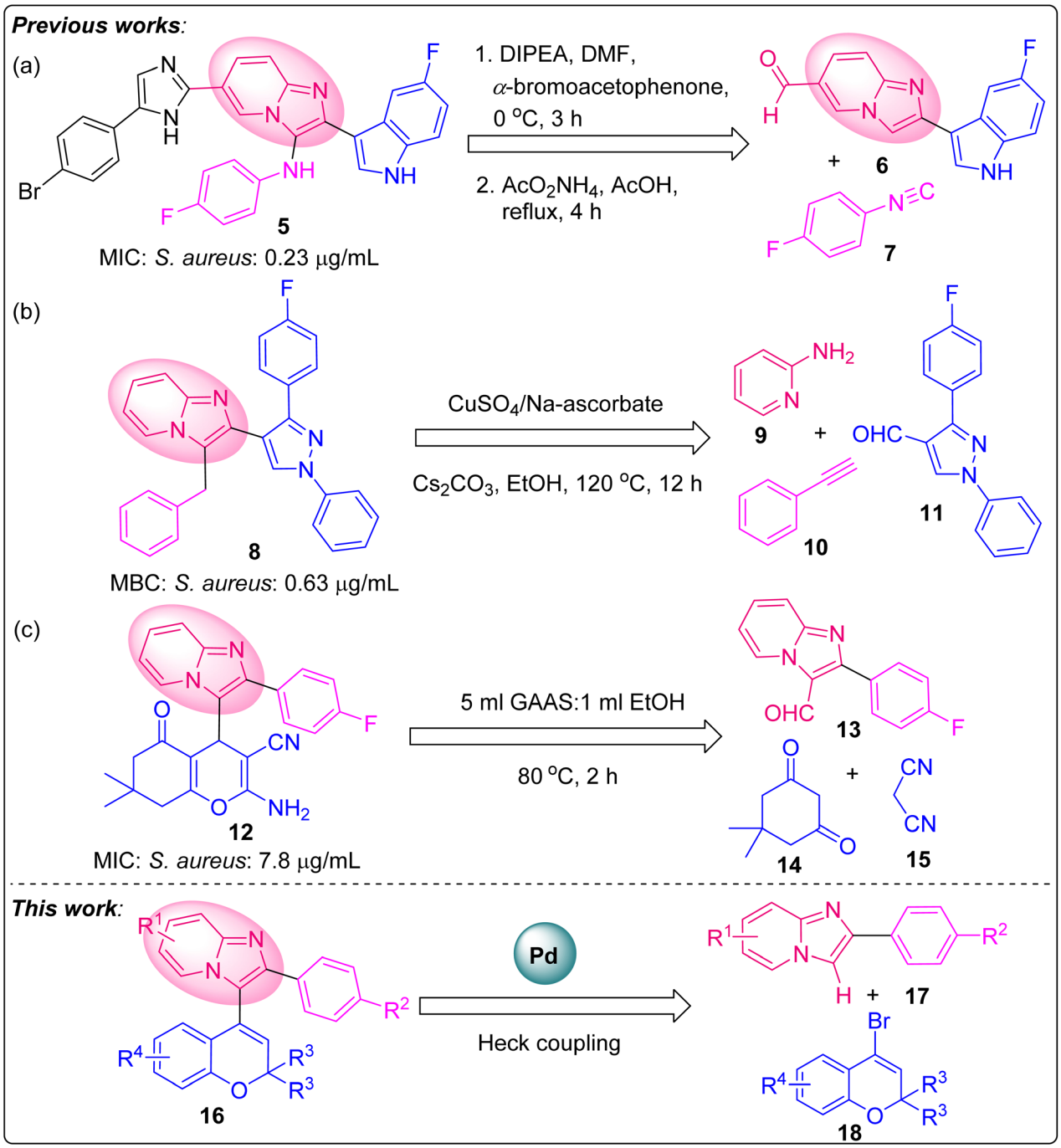

Fig. 2 Imidazo[1,2-*a*]pyridine-based molecules exhibiting potent antibacterial activity against Gram-positive *S. aureus*.

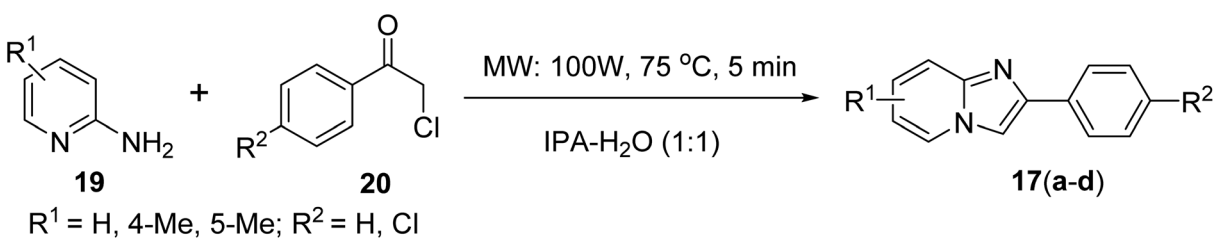

Scheme 1 Synthesis of phenylimidazo[1,2-*a*]pyridine derivatives **17(a–d)**.

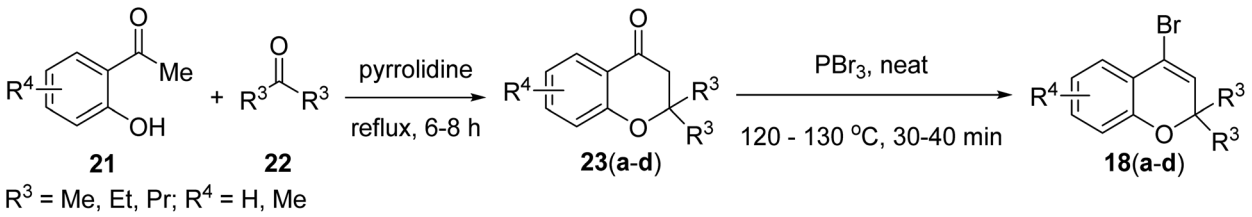

Scheme 2 Synthesis of 4-bromo-2,2-dialkyl-substituted 2*H*-chromenes **18(a–d)**.

due to the different environments. All other protons and carbons appeared in their respective positions, which clearly indicated the formation of phenylimidazo[1,2-*a*]pyridine-chromene derivatives. The HRMS analysis of compound **16a** showed an experimental value of $[M + H]^+$ at 353.1616 compared to the calculated value of 353.1654, which confirmed the formation of product **16a** (Fig. 3).

After optimizing the reaction conditions and characterization of **16a** by ^1H, ^{13}C NMR, and HRMS, we wished to expand the substrate scope of the phenylimidazo[1,2-*a*]pyridine-chromene derivatives. Consequently, the substituted imidazo[1,2-*a*]pyridines **17(a–d)** were coupled with four different 4-bromo-2,2-dialkyl substituted 2*H*-chromene derivatives **18(a–d)**, furnishing 21 phenylimidazo[1,2-*a*]pyridine-chromene derivatives **16(a–u)** with good yields, as shown in Table 2.

It was found that the yield of the product depended on the various substituents at the different positions. In the chromene core, whenever the alkyl chain length at the 2-position increased, the yield gradually decreased. Trisubstituted methyl groups in the chromene ring **16(g–i)** also provided better yields than for the 2,2-dimethyl-substituted chromene. In the case of imidazo[1,2-*a*]pyridine, whenever there was chloro substitution in the benzene ring, *i.e.*, **16(d–i)**, **16(m–o)**, and **16(s–u)**, the yields were better than the unsubstituted ones, *i.e.*, **16a**, **16j**, and **16p**. Whenever the methyl substituents was in the 7th position of imidazo[1,2-*a*]pyridine (**16b**, **16e**, **16h**, **16k**, **16n**, **16q**, and **16t**), the yield was better than the 6th-positioned methyl imidazo[1,2-*a*]pyridine (**16c**, **16f**, **16i**, **16l**, **16o**, **16r**, and **16u**). We also tried the reaction with keeping the methyl group in the 5th position of imidazo[1,2-*a*]pyridine, but a series of spots developed, preventing us from separating out the product.

2.1.3. X-ray crystallographic analysis. The confirmation of the configuration of compound **16e** was achieved through single-crystal X-ray analysis, and then the configurations of all other molecules were subsequently based on this analysis, as elucidated in Fig. 4.[22]

2.2 Biological studies

2.2.1. Antibacterial evaluation. After synthesizing the series of compounds 3-(2,2-dialkyl-2*H*-chromen-4-yl)-2-phenylimidazo[1,2-*a*]pyridine **16(a–u)**, the agar well diffusion method was used to investigate their *in vitro* antibacterial activity against the Gram-negative pathogenic bacteria *E. coli* and Gram-positive bacteria *S. aureus*, concurrently with a study of their zone of inhibition (ZI) using an assay and their minimum inhibitory concentration (MIC) values. Compared to the standard drug gentamicin, compounds **16a**, **16b**, **16c**, **16d**, **16f**, **16g**, **16h**, **16i**, and **16n** exhibited notable antibacterial activities against both strains *i.e.*, *E. coli* and *S. aureus*. Among all the synthesized compounds, the most potent compound was found to be **16h** with a ZI of 19 mm and an MIC of 10 μg mL^{-1} for *E. coli* and *S. aureus*. The second most potent compound was **16n**, which showed a ZI of 19 mm and MIC of 10 μg mL^{-1} and ZI of 17 mm and MIC of 20 μg mL^{-1} for *E. coli* and *S. aureus*, respectively. Compound **16r** had the lowest potency, with a ZI of 13 mm and MIC of 40 μg mL^{-1} and ZI of 11 mm and MIC of 60

Table 1 Exploring the reaction conditions for the Heck coupling reaction for the synthesis of **16a**

					Conventional method			Microwave irradiation method			
Entry[a]	Coupling reagent	Base	Solvent	Ligand	Temp. (°C)	Time (h)	Yield[b] (%)	MW (W)	Temp (°C)	Time (min)	Yield[b] (%)
1	$Pd(OAc)_2$	—	1,4-Dioxane/EtOH (2 : 1)	TPP	100	3	—	100	100	30	—
2	$Pd(PPh)_3Cl_2$	Et_3N	DMF	—	100	4	11	50	80	30	44
3	$Pd(PPh)_3Cl_2$	K_3PO_4	DMF	—	100	4	24	70	90	30	36
4	$Pd(PPh)_3Cl_2$	K_2CO_3	DMF	—	100	4	27	90	100	30	30
5	$Pd(PPh)_3Cl_2$	NaOAc	DMF	—	100	4	10	120	120	30	32
6	$Pd(OAc)_2$	Et_3N	DMF	TPP	120	4	24	80	100	20	40
7	$Pd(OAc)_2$	K_3PO_4	DMF	—	100	3	31	100	120	20	40
8	**$Pd(OAc)_2$**	**K_2CO_3**	**DMF**	—	**120**	**2**	**76**	80	100	10	75
9	$Pd(OAc)_2$	NaOAc	DMF	—	100	4	23	90	100	20	65
10	**$Pd(OAc)_2$**	**K_2CO_3**	**DMF**	—	150	5	54	**100**	**120**	**20**	**88**
11	$Pd(OAc)_2$	K_2CO_3	CH_3CN	—	80	4	36	100	120	20	70

[a] Reaction conditions: **17a** (1 mmol), **18a** (3 mmol), Pd catalyst (0.1 equiv.), K_2CO_3 as base (3 equiv.), and solvent (3–4 mL). [b] Isolated yield, MW: microwave.

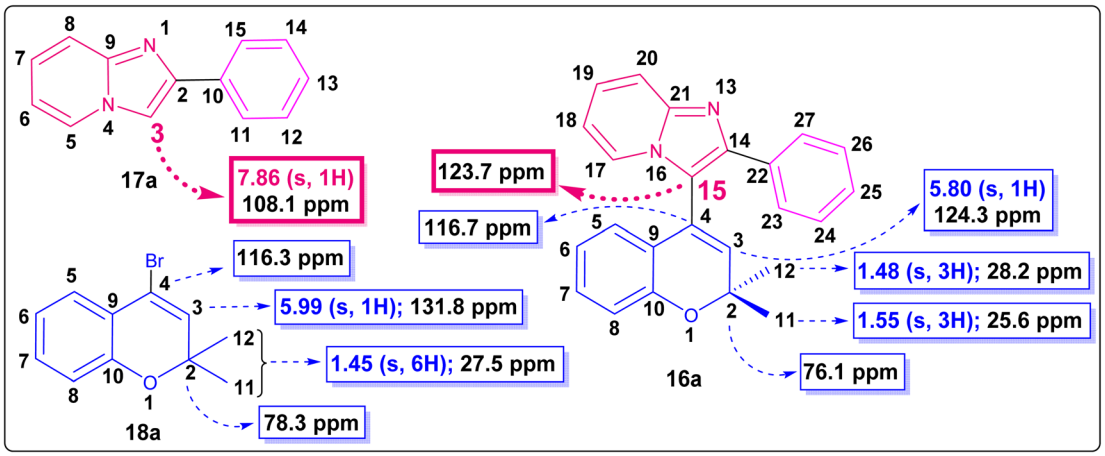

Fig. 3 ^{1}H and ^{13}C NMR data analysis of **16a**.

μg mL^{-1} for *E. coli* and *S. aureus*, respectively (Table 2). The ZI and MIC values of the synthesized compounds are graphically depicted in Fig. 5 and 6, respectively.

2.2.2. Structure–activity relationship (SAR studies). The antibacterial activity screening results of the tested hybrids can be used to summarize the structure–activity relationship. This relationship emphasizes the importance of the substituents associated with the hybrid structure (Fig. 7). The methyl group in the R^1 position attached to the imidazo[1,2-*a*]pyridine core at position 6/7 (**16b–c**, **16e–f**, **16h–i**, **16k–l**, **16n–o**, **16q–r**, **16t–u**) increased the antibacterial activity. Also, the chloro substitution in the R^2 position in the benzene ring of the imidazo[1,2-*a*] pyridine (**16d–i**, **16m–o**, **16s–u**) increased the antibacterial activity. The two methyl groups in the R^3 position in the chromene ring increased the antibacterial activity (**16a–i**). However, when the alkyl chain length increased from Me to Et (**16j–o**) to Pr (**16p–u**), the antibacterial activity decreased. The methyl group in the R^4 position in the chromene ring also increased the antibacterial activity (**16g–i**). Trisubstituted methyl groups in the chromene ring overall also increased the antibacterial activity, with **16h** being the most potent. Hence, compound **16h**, which has –Cl in the phenyl ring of the imidazo[1,2-*a*]pyridine moiety and trisubstituted methyl in the chromene ring, was found to be the most potent compound.

Table 2 Antibacterial activities of the newly synthesized derivatives 16(a–u)[a]

	E. coli		*S. aureus*	
Compound code	ZI (mm)	MIC (μg ml^{-1})	ZI (mm)	MIC (μg ml^{-1})
16a	17	20	16	30
16b	17	20	15	30
16c	16	20	16	30
16d	17	20	17	20
16e	15	30	15	30
16f	17	20	17	20
16g	16	20	17	20
16h	**19**	**10**	**19**	**10**
16i	16	20	17	20
16j	17	20	14	40
16k	15	30	15	30
16l	15	30	13	40
16m	15	30	15	30
16n	**19**	**10**	**17**	**20**
16o	15	30	15	30
16p	13	40	12	50
16q	13	40	13	40
16r	13	40	11	60
16s	17	20	14	40
16t	13	40	14	40
16u	15	30	16	30
*Standard	20	10	20	10

[a] ZI: zone of inhibition, MIC: minimum inhibitory concentration, *standard drug: gentamicin.

2.2.3. Computational studies. In order to obtain insights into the mechanism of inhibition of DNA gyrase receptor, molecular docking experiments of the synthesized derivatives **16(a–u)** were performed against bacterial DNA gyrases of *E. coli* (PDB ID: 1AJ6) and *S. aureus* (PDB ID: 3G7B). With ligand–protein binding energies ranging from −7.1 kcal mol^{-1} to −8.7 kcal mol^{-1} for the *E. coli* DNA gyrase and −6.6 kcal mol^{-1} to −8.7 kcal mol^{-1} for the *S. aureus* DNA gyrase, the study's findings showed that the ligands of the synthesized compounds had good binding interactions with the bacterial proteins. According to the docking investigations, all of the synthesized compounds displayed a more robust binding relationship with the *E. coli* DNA gyrase than with the *S. aureus* DNA gyrase. Compound **16h** demonstrated strong binding interactions with DNA gyrases from both *E. coli* (PDB ID: 1AJ6) and *S. aureus* (PDB ID: 3G7B), each exhibiting an affinity of −8.7 kcal mol^{-1}. Compound **16r** on the other hand, showed the least affinity for binding to DNA gyrases from *E. coli* and *S. aureus*, with docking scores of −7.3 and −6.6 kcal mol^{-1}, respectively. The docked complexes engaged with the amino acids of DNA gyrase through interactions like van der Waals, π-donor hydrogen bond, π–σ interaction, alkyl, π-alkyl, π-cation, and π-anion. Table 3 displays the binding interactions and docking scores.

Compound **16h**, which was found to be the most potent, demonstrated a range of ligand–protein interactions, such as van

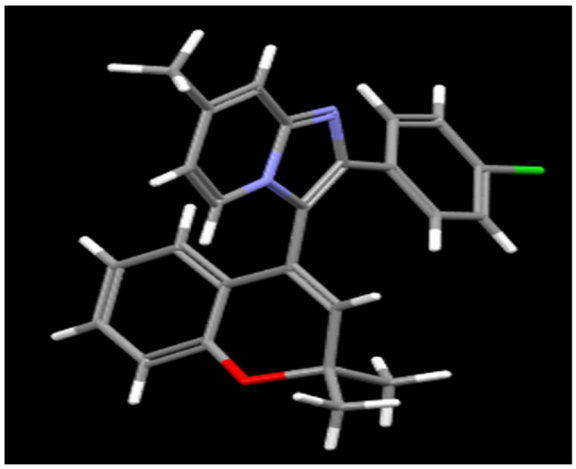

Fig. 4 Single-crystal X-ray diagram of 2-(4-chlorophenyl)-3-(2,2-dimethyl-2*H*-chromen-4-yl)-7-methylimidazo[1,2-*a*]pyridine **16e** (CCDC 2347891).

der Waals interactions with the amino acid residues ASP 34, ASP 38, MET 79, VAL 32, THR 142, ALA 36, ASP 62, GLU 39, ASN 35, VAL 97, ALA 74, VAL 81, SER 98, HIS 83, GLY 96, and GLY 94, alkyl and π-alkyl interactions with VAL 144, PRO 68, ALA 84, and π–σ interactions with ILE 67 and ILE 78. According to these findings, these results show the effective insertion of **16h** into the active cavities of *E. coli* DNA gyrase. Similarly, compound **16h** also demonstrated a strong binding affinity with an energy of −8.7 kcal mol^{-1}, and was retained within the active pockets of *S. aureus* DNA gyrase enzymes through van der Waals interactions with ARG 98, GLY 62, ASP 58, THR 127, SER 32, ASN 31, ASP 34, π-cation and π-anion interactions with ARG 61, GLU 35, and alkyl and π-alkyl interactions with ILE 79, PRO 64, ILE 63, and ALA 38. According to the 3D-interaction analysis of the synthesized phenylimidazo[1,2-*a*]pyridine-chromene analogues, compound **16h** containing –Cl in the phenyl ring of the imidazo[1,2-*a*]pyridine moiety along with trisubstituted methyl in the chromene ring exhibited the highest level of DNA gyrase-inhibitory activity. It also displayed strong antibacterial activity. Fig. 8 and 9 display the corresponding docking images and 3D interactions of compound **16h** against DNA gyrases from *E. coli* (PDB ID: 1AJ6) and *S. aureus* (PDB ID: 3G7B), respectively.

2.2.4. Estimation of the physicochemical, pharmacokinetic, and ADME properties. Bioavailability is a crucial factor in drug development, as a pharmaceutical candidate must reach its target in the body at the required concentration to be effective, but without causing adverse effects. *In silico* ADMET predictions can help identify promising compounds and reduce late-stage toxicity. Therefore, to assess the physicochemical and pharmacokinetic properties, ADME predictions were made for all the synthesized compounds and the standard drug gentamicin using the SwissADME tool (Table 4).[23] According to Lipinski's "rule of 5," an orally active drug should violate no more than one of these criteria: MW < 500 Da, HBD < 5, HBA < 10, *M* log *P* < 4.15, and BS = 0.55. Additional factors like ROTB < 9 and TPSA < 140 $Å^2$ also influence the bioavailability. The topological polar surface area (TPSA), which is inversely related to the percentage absorption (%ABS = 109 − 0.345 × TPSA), can be used as an alternative to counting the hydrogen-bonding groups for estimating absorption. Here, compound **16a** showed zero violations, while gentamicin violated two. Most compounds in the series violated at least one rule, making them suitable drug-like candidates. Five compounds exhibited high gastrointestinal absorption, suggesting effective absorption, with all the compounds achieving systemic circulation (bioavailability = 0.55).

Furthermore, the physicochemical properties and medicinal chemistry of the most potent antibacterial compound, **16h**, were assessed using ADMETlab 3.0 to evaluate its ADMET (absorption, distribution, metabolism, excretion, and toxicity) profile, which can help in determining its drug-likeness (Table 5).[24,25]

The ADMET characteristics of the most potent compound **16h** are presented in Table 6. The compound demonstrated favourable results in terms of human intestinal absorption (HIA) and the predicted bioavailability ($F_{50\%}$) score. Regarding the metabolism, the Caco-2 permeability value was −4.578 log

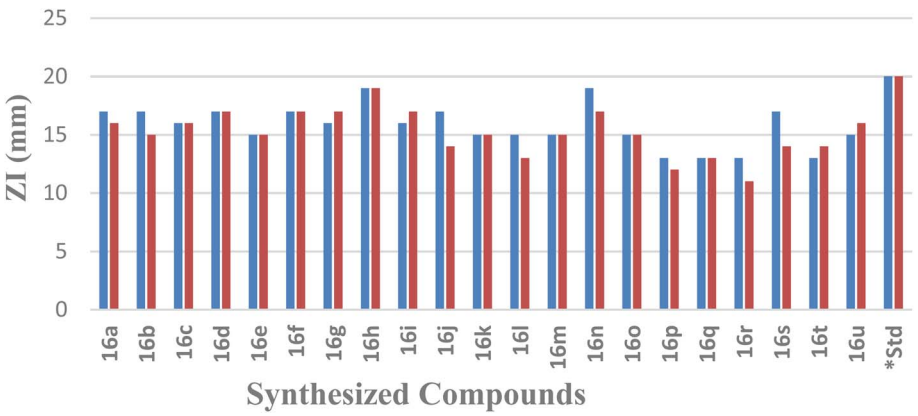

Fig. 5 Graphical representation of the inhibitory antimicrobial action by ZI assay of the synthesized 3-(2,2-dialkyl-2*H*-chromen-4-yl)-2-phenylimidazo[1,2-*a*]pyridine derivatives **16(a–u)** assessed with the standard drug gentamicin. The blue and red colours indicate the inhibition of *E. coli* and *S. aureus*, respectively.

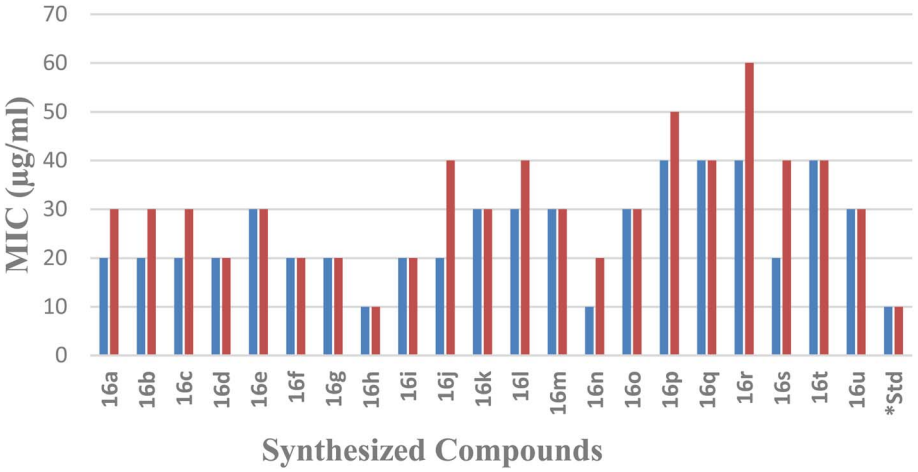

Fig. 6 Graphical representation of the *in vitro* antimicrobial (MIC) assay results for the synthesized 3-(2,2-dialkyl-2*H*-chromen-4-yl)-2-phenylimidazo[1,2-*a*]pyridine derivatives **16(a–u)** assessed with the standard drug gentamicin. The blue and red colours indicate the inhibition of *E. coli* and *S. aureus*, respectively.

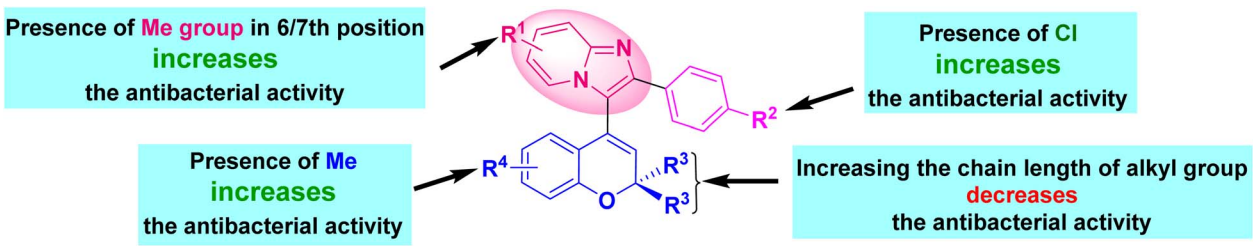

Fig. 7 Pictorial representation of the SAR summary for the phenylimidazo[1,2-*a*]pyridine-chromene hybrids **16(a–u)**.

units. The prediction indicated a relatively low metabolic clearance (CL = 4.967 mL min^{-1} kg^{-1}) with a short half-life ($T_{1/2}$ = 0.541 h). Therefore, based on the ADMET analysis, compound **16h** is expected to be safe and is unlikely to cause eye corrosion or irritation.

3. Conclusion

In conclusion, a series of 21 novel 3-(2,2-dialkyl-2*H*-chromen-4-yl)-2-phenylimidazo[1,2-*a*]pyridine derivatives were produced in good to excellent yields by a proficient palladium-catalyzed cross-coupling reaction under microwave irradiation. The antibacterial activities of all these compounds were assessed *in vitro* using the agar well diffusion method against human pathogenic Gram-negative *E. coli* and Gram-positive *S. aureus* bacteria, and their MIC values were determined. Compound **16h** displayed ZI values of 19 mm and MIC values of 10 µg mL^{-1} in both *E. coli* and *S. aureus*, in comparison to the standard drug gentamicin. It also strongly inhibited DNA gyrase *in silico* with a binding affinity of −8.7 kcal mol^{-1}. As inferred from the structure–activity relationships based on molecular docking studies and their strong antibacterial properties, these novel phenylimidazo[1,2-*a*]pyridine-chromene derivatives may be powerful antibacterial agents for use in the near future. Therefore, we anticipate that our work will aid in the creation of novel heterocyclic scaffolds by the synthetic fraternity, with a focus on producing effective antibacterial candidates for drug development.

4. Experimental section

4.1 Chemistry

4.1.1. General methods. All the reagents and solvents were purchased from commercial suppliers. Chemicals such as 2-aminopyridines, 4- and 5-Me-substituted-2-aminopyridines, 2-haloacetophenones, 2′-hydroxy-acetophenone, pyrrolidine, and aliphatic ketones reagents were purchased from Sigma-Aldrich or TCI and were used without further purification. The progress of the reactions of imidazo[1,2-*a*]pyridines, 2*H*-chromenes, and the novel hybrid molecules was monitored by thin-layer chromatography using silica gel $60F_{254}$ (TLC, Merck). The compounds were purified by column chromatography. ^{1}H NMR and ^{13}C NMR were done to confirm the structure of the product. The ^{1}H NMR spectra were acquired on a JEOL FT NMR spectrometer at 400 MHz. The ^{13}C NMR spectra were acquired on a JEOL FT NMR at 100 MHz. All the NMR spectra were acquired in $CDCl_3$ at 27 °C with TMS as the internal reference. Chemical shifts (δ) were presented in ppm units and the coupling constants (J) in Hertz (Hz). Signal multiplicity was expressed by the following abbreviations: s (singlet), d (doublet), dd (doublet

Table 3 Docking score and binding interactions of the synthesized compounds **16(a–u)** with amino acid residues of DNA gyrase

	E. coli DNA gyrase (PDB ID: 1AJ6)		*S. aureus* DNA gyrase (PDB ID: 3G7B)	
Compound code	Binding affinity (kcal mol^{-1})	Residues showing interaction	Binding affinity (kcal mol^{-1})	Residues showing interaction
16a	−8.7	ASP 34, ASP 38, GLU 31, ASN 35, ILE 67, PRO 68, VAL 97, ILE 78, SER 98, ALA 84, VAL 81, GLY 96, HIS 83, LEU 82, LYS 87, PHE 88, GLY 86, GLY 94	−8.1	ILE 129, ASN 31, ILE 79, THR 127, SER 32, ASP 58, GLY 62, ILE 63, GLU 35, PRO 64, ARG 98, ARG 61, ASP 34
16b	−8.6	ALA 42, ARG 65, ASP 38, GLU 39, ILE 67, ALA 36, ASP 62, THR 142, ASP 34, ASN 35, GLY 94, GLU 31, GLY 96, VAL 97, ILE 78	−7.5	ASN 31, ASP 34, GLY 62, ARG 61, GLU 35, ARG 98, PRO 64, ILE 63, THR 127, SER 32, ASP 58, ILE 129, ILE 79, LEU 80, SER 83
16c	−8.5	ALA 42, ASP 38, ARG 65, GLU 39, ILE 67, ALA 36, ASP 62, THR 142, ASP 34, ASN 35, MET 79, GLY 94, GLU 31, VAL 97, GLY 96, ILE 78	−7.6	ILE 79, ASN 31, SER 32, ASP 58, THR 127, ILE 63, GLY 62, GLU 35, PRO 64, ARG 98, ARG 61, ALA 38, ASP 34
16d	−8.4	ILE 67, ASP 62, THR 142, ASN 35, VAL 97, ILE 78, GLY 96, HIS 83, ALA 84, ASP 38, ALA 42, GLU 39, ARG 65, PRO 68	−8.1	ILE 28, ILE 79, ILE 129, THR 127, ASN 31, SER 32, ASP 58, ILE 63, GLY 62, GLU 35, PRO 64, ARG 98, ARG 61, ASP 34
16e	−7.2	PRO 68, ILE 67, ARG 65, MET 79, ASN 35, THR 142, VAL 144, VAL 97, VAL 32, ASP 62, ALA 36, ILE 78, GLU 39, GLY 96, ASP 34, ASP 38	−7.6	ILE 79, ARG 98, ARG 61, PRO 64, GLY 62, GLU 35, ILE 63, THR 127, SER 32, ASP 58, ASN 31, ALA 38, ASP 34
16f	−8.4	ILE 67, GLU 39, ARG 65, ASP 38, ALA 42, ASP 34, GLY 94, GLU 31, ASN 35, GLY 96, VAL 97, ILE 78, THR 142, MET 79	−8.0	PRO 64, GLU 35, ILE 63, ARG 61, GLY 62, THR 127, ASP 58, SER 32, ILE 129, ILE 28, ASN 31, LEU 80, SER 83, ILE 79, ASP 34
16g	−8.1	ALA 42, ASP 38, ALA 84, HIS 83, GLY 96, SER 98, VAL 97, ILE 78, GLU 39, ASN 35, THR 142, ASP 62, ILE 67, ALA 36, PRO 68, ARG 65	−8.4	ASP 34, ALA 38, GLU 35, ARG 98, PRO 64, GLY 62, ARG 61, ASP 58, ILE 63, THR 127, SER 32, ILE 79, ASN 31
16h	**−8.7**	**ASP 34, ASP 38, VAL 144, MET 79, VAL 32, THR 142, ALA 36, ASP 62, GLU 39, ASN 35, ILE 67, VAL 97, ALA 74, PRO 68, ILE 78, VAL 81, SER 98, HIS 83, ALA 84, GLY 96, GLY 94**	**−8.7**	**ARG 61, ARG 98, PRO 64, GLY 62, GLU 35, ILE 63, ASP 58, THR 127, SER 32, ASN 31, ASP 34, ALA 38, ILE A:79**
16i	−8.4	ASP 38, ARG 65, ALA 42, HIS 83, ALA 84, GLY 96, VAL 97, SER 98, ILE 78, GLU 39, ASN 35, THR 142, ILE 67, ASP 62, ALA 36, GLY 66, ALA 75, GLY 64, PRO 68, ALA 74	−8.5	ILE 79, ASN 31, ILE 129, SER 32, ASP 58, THR 127, GLY 62, ILE 63, GLU 35, PRO 64, ARG 98, ARG 61, ALA 38, ASP 34
16j	−8.5	VAL 97, SER 98, GLY 96, ILE 78, ARG 65, PRO 68, GLU 39, GLY 66, ILE 67, ASP 62, THR 142, ALA 36, ASN 35, VAL 32, VAL 144, MET 79, ASP 38	−7.1	ILE 79, PRO 64, ARG 98, ARG 61, GLY 62, GLU 35, ILE 63, THR 127, ASP 58, ASN 31, ALA 38, ASP 34
16k	−7.7	PRO 68, ALA 84, HIS 83, ILE 78, GLY 96, ASN 35, VAL 97, ILE 67, MET 79, VAL 144, THR 142, ASP 62, ALA 36, ASP 38, ALA 42, GLU 39, GLY 66, ARG 65	−7.7	PRO 64, ARG 98, ARG 61, GLY 62, GLU 35, ILE 63, ASP 58, SER 32, THR 127, ILE 129, ASP 34, ALA 38, ASN 31, ILE 79

Table 3 (*Contd.*)

Compound code	*E. coli* DNA gyrase (PDB ID: 1AJ6)		*S. aureus* DNA gyrase (PDB ID: 3G7B)	
	Binding affinity (kcal mol^{-1})	Residues showing interaction	Binding affinity (kcal mol^{-1})	Residues showing interaction
16l	−8.0	ILE 78, PRO 68, ILE 67, GLU 39, ALA 36, ASP 62, THR 142, ASP 38, ASN 35, VAL 144, MET 79, HIS 83, ALA 84, VAL 97, VAL 81, SER 98, GLY 96	−7.5	ILE 79, THR 127, ILE 63, GLU 35, ASP 34, ASN 31, ASP 30, GLU 27, VAL 84, ILE 129, SER 83, SER 82, LEU 80, ILE 28
16m	−8.0	PRO 68, GLY 66, ALA 36, ASP 62, ILE 67, THR 142, VAL 144, MET 79, ASN 35, VAL 97, ILE 78, GLY 96, ALA 84, ASP 38, ARG 65, GLU 39, ALA 42	−7.5	ILE 79, ARG 61, ARG 98, PRO 64, GLU 35, ASN 31, ILE 63, THR 127, GLY 62, ILE 129, SER 32, ASP 34, ASP 58
16n	−8.7	ASP 34, ASP 38, GLU 31, ASN 35, ILE 67, ILE 78, MET 79, VAL 97, PRO 68, SER 98, VAL 81, ALA 84, GLY 96, HIS 83, LEU 82, GLY 86, LYS 87, PHE 88, GLY 94	−7.8	ILE 79, ASP 34, ILE 63, SER 32, GLU 35, ASN 31, THR 127, GLU 27, ILE 129, ILE 28, LEU 80, VAL 85, VAL 84, SER 83, SER 82
16o	−8.1	PRO 68, ARG 65, GLU 39, GLY 66, ILE 67, ASP 62, ALA 36, THR 142, ALA 42, VAL 32, ASP 38, ASN 35, VAL 97, ILE 78	−7.8	ARG 98, GLU 35, PRO 64, GLY 62, ARG 61, THR 127, ASP 58, ASN 31, SER 32, ILE 63, ILE 79, ASP 34
16p	−8.0	ALA 42, ASP 38, ARG 65, ILE 67, GLU 39, ASP 62, THR 142, ASP 34, ASN 35, GLU 31, GLY 94, VAL 97, GLY 96, SER 98, ALA 84, ILE 78, HIS 83	−6.9	ALA 38, ASP 34, ARG 61, ARG 98, PRO 64, GLU 35, GLY 62, ILE 63, ILE A:79, GLY 60, ASN 31, SER 32, ASP 58, THR 127
16q	−7.2	ALA 42, ASP 38, ARG 65, GLU 39, GLY 66, ASP 62, THR 142, ILE 67, ASN 35, ILE 78, VAL 97, GLY 96, PRO 68, ALA 74	−7.2	ARG 98, ARG 61, GLU 35, ILE 63, PRO 64, GLY 62, GLY 126, ASN 31, GLY 60, ASP 58, THR 127, SER 32, ASP 34, ALA 38, ILE 79
16r	−7.3	GLY 66, PRO 68, ALA 84, ILE 78, ILE 67, THR 142, ASN 35, VAL 97, GLY 96, MET 79, VAL 144, ASP 62, ALA 36, ASP 38, ALA 42, ARG 65, GLU 39	−6.6	ILE 129, THR 127, ASP 58, ALA 38, SER 32, ASP 34, ILE 79, ARG 61, ARG 98, PRO 64, GLU 35, ASN A:31, GLY 62, ILE 63
16s	−8.1	PRO 68, GLY 66, ILE 67, ALA 36, ASP 62, THR 142, ASN 35, VAL 97, GLY 96, HIS 83, ALA 84, ILE 78, ASP 38, ALA 42, ALA 74	−6.9	ILE 79, ARG 61, PRO 64, ARG 98, GLU 35, GLY 62, ILE 63, SER 32, THR 127, ASP 58, ASP 34, ALA 38, ASN 31
16t	−7.7	ILE 78, VAL 97, VAL 81, HIS 83, ALA 84, GLY 96, ASN 35, GLU 31, GLY 94, ARG 65, ASP 34, PRO 68, GLY 66, THR 142, ILE 67, GLU 39, ALA 36, ASP 38, ALA 42	−7.4	ASP 34, ALA 38, ILE 79, ASN 31, ILE 63, SER 32, GLU 35, GLY 62, THR 127, ASP 58, GLY 126, GLY 60, PRO 64, ARG 61, LEU 37
16u	−7.1	GLY 66, GLY 64, PRO 68, ASP 62, THR 142, ILE 67, ASN 35, ILE 78, ALA 84, ASP 38, ALA 42, ARG 65, GLU 39	−7.5	PRO 64, ARG 61, ARG 98, GLU 35, GLY 62, THR 127, ASP 58, SER 32, ASP 34, ASN 31, ILE 63, ILE 79

of doublets), m (multiplet). However, the exact masses of these compounds were further confirmed by HRMS spectrometry. Mass spectra were acquired on a Micromass Q-ToF high-resolution mass spectrometer equipped with electrospray ionization (ESI) on a Masslynx 4.0 data acquisition system. ESI was used in the +ve ionization mode. Melting points were determined on SMP-10 digital apparatus and are presented uncorrected.

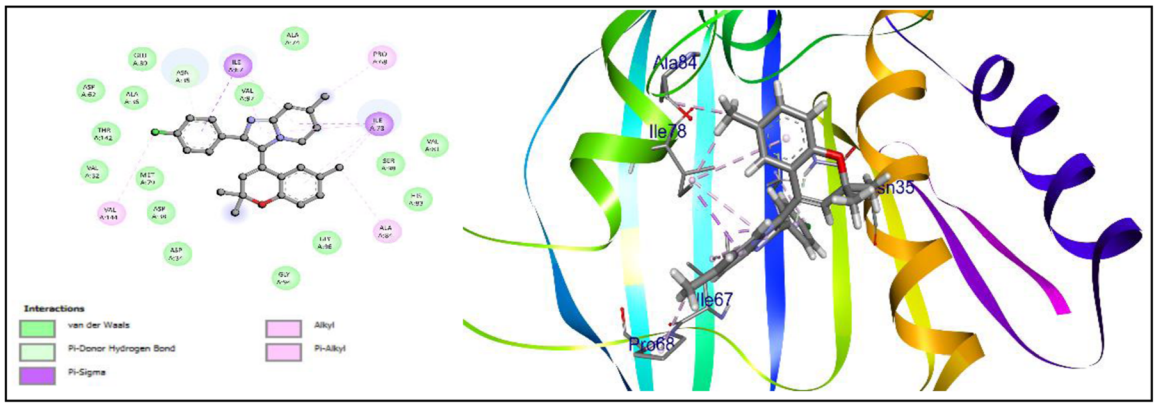

Fig. 8 Docking interaction and 3D binding image of compound **16h** with *E. coli* DNA gyrase (PDB ID: 1AJ6).

4.1.2. General procedure for the synthesis of the imidazo[1,2-*a*]pyridine derivatives 17(a–d). A mixture of 2-chloroacetophenone/2,4′-dichloroacetophenone (1.0 equiv.) and 4-Me/5-Me substituted 2-aminopyridine (2.0 equiv.) was added to a 2 mL solution of H_2O–IPA (1 : 1). The reaction mixture was irradiated under microwave heating at 100 W for 5 min at 75 °C. The progress of the reaction was monitored by TLC. After completion of the reaction, the reaction mixture was ice cooled to give a solidified product. The filtered solid product was then recrystallised from IPA to afford the pure desired 2,4′-dichloroimidazo[1,2-*a*]pyridine derivatives. However, in the case of 2-chloroacetophenone, the reaction mixture was extracted with ethyl acetate (10 mL, twice), then the combined organic layer was treated over anhydrous Na_2SO_4. The combined filtrate was subjected to evaporation to obtain the crude compound, which was purified by silica gel column chromatography (60–120 mesh) using 30% ethyl acetate in hexane as the eluent to obtain the corresponding phenyl-substituted imidazo[1,2-*a*]pyridine as product **17** (Scheme 1).[18,19]

4.1.3. General procedure for the synthesis of the 4-bromo-2,2-dialkyl-substituted 2*H*-chromene derivatives 18(a–d). In a clean and dry 250 mL round-bottom flask, 2′-hydroxy acetophenone (1 equiv.), dialkyl ketones (3 equiv.), and pyrrolidine (0.5 equiv.) were added and the reaction mixture was stirred at room temperature for 6 h at 100 °C. The progress of the reaction was monitored by TLC. After completion of the reaction, the reaction mixture was extracted with ethyl acetate and water. The organic layers were washed with brine, dried over anhydrous Na_2SO_4, and then evaporated by a rotary evaporator. The crude product was purified by column chromatography to afford the desired 2,2-dialkyl substituted chromone products **23(a–d)**. In the subsequent step, the mixture of the obtained chromone (1 equiv.) and PBr_3 (4 equiv.) was heated for 30 min at 120–130 °C. Afterwards, the reaction mixture was allowed to cool to room temperature, then diluted with ice water and extracted with ethyl acetate. The ethyl acetate layers were further washed with brine and dried over anhydrous Na_2SO_4. The organic layers were evaporated and the crude products were purified by column chromatography (60–120 mesh silica mesh) using hexane as the eluent to obtain the desired 4-bromo-2,2-dialkyl-substituted 2*H*-chromene derivatives **18(a–d)** (Scheme 2).[20,21]

4.1.4. General procedure for the synthesis of the 3-(2,2-dialkyl-2*H*-chromen-4-yl)-2-phenylimidazo[1,2-*a*]pyridine derivatives 16(a–u). The cross-couplings of various 4-bromo-2,2-dialkyl substituted 2*H*-chromenes (2 equiv.) and 2-phenylimidazo[1,2-*a*]pyridine (1 equiv.)/2-phenylchloroimidazo[1,2-*a*]

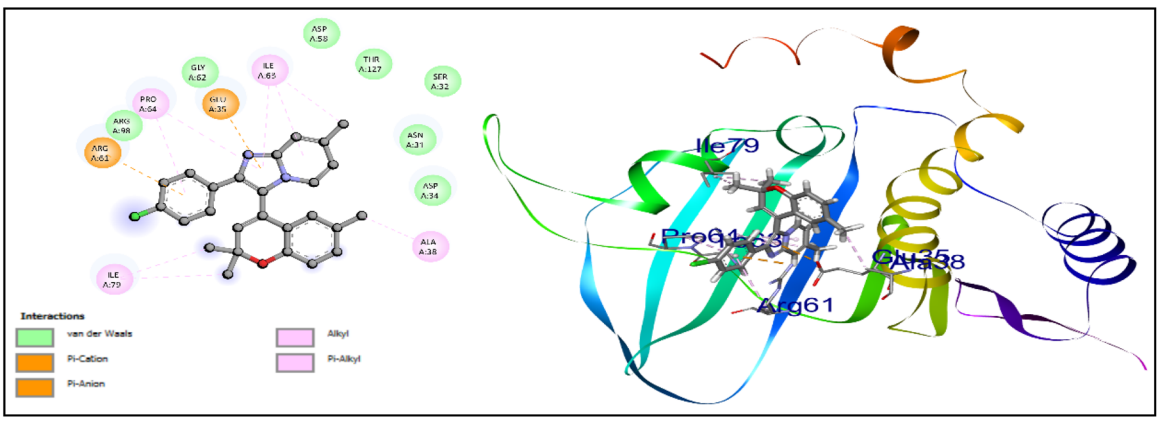

Fig. 9 Docking interaction and 3D binding image of compound **16h** with *S. aureus* DNA gyrase (PDB ID: 3G7B).

Table 4 Calculated Lipinski's 'rule of 5' for the **16(a–u)** derivatives utilizing the SwissADME free web tool

	MW[a]	*M* log *P*[b]	ROTB[c]	HBA[d]	HBD[e]	TPSA[f]	Violations	GI abs[g]	BS[h]
16a	352.43	3.95	2	2	0	26.53	0	High	0.55
16b	366.45	4.15	2	2	0	26.53	1	High	0.55
16c	366.45	4.15	2	2	0	26.53	1	High	0.55
16d	386.87	4.42	2	2	0	26.53	1	High	0.55
16e	400.9	4.63	2	2	0	26.53	1	Low	0.55
16f	400.9	4.63	2	2	0	26.53	1	Low	0.55
16g	400.9	4.63	2	2	0	26.53	1	Low	0.55
16h	414.93	4.83	2	2	0	26.53	1	Low	0.55
16i	414.93	4.83	2	2	0	26.53	1	Low	0.55
16j	380.48	4.36	4	2	0	26.53	1	High	0.55
16k	394.51	4.56	4	2	0	26.53	1	Low	0.55
16l	394.51	4.56	4	2	0	26.53	1	Low	0.55
16m	414.93	4.83	4	2	0	26.53	1	Low	0.55
16n	428.95	5.03	4	2	0	26.53	1	Low	0.55
16o	428.95	5.03	4	2	0	26.53	1	Low	0.55
16p	408.53	4.76	6	2	0	26.53	1	Low	0.55
16q	422.56	4.95	6	2	0	26.53	1	Low	0.55
16r	422.56	4.95	6	2	0	26.53	1	Low	0.55
16s	442.98	5.22	6	2	0	26.53	1	Low	0.55
16t	457.01	5.41	6	2	0	26.53	1	Low	0.55
16u	457.01	5.41	6	2	0	26.53	1	Low	0.55
*Std	477.6	−2.92	7	12	8	199.73	2	Low	0.17

[a] Molecular weight in g mol^{-1}. [b] Partition coefficient (lipophilicity). [c] Number of rotatable bonds. [d] Number of H-bond acceptors. [e] Number of H-bond donors. [f] Topological polar surface area in Å^2. [g] Gastrointestinal absorption. [h] Bioavailability score, *std: gentamicin as the standard.

pyridine (1 equiv.) were carried out in anhydrous DMF solvent using K_2CO_3 (3 equiv.), $Pd(OAc)_2$ (0.1 equiv.) under conventional heating conditions for 1.5–2 h at 120 °C. The progress of the reaction was monitored by TLC. After completion of the reaction, the reaction mixture was diluted with water and extracted with ethyl acetate. The ethyl acetate layers were further washed with brine and dried over anhydrous Na_2SO_4. The organic layer was evaporated and the crude products were purified by column chromatography using EtOAc and hexane (2 : 8) as the eluent. Further, the same coupling reaction was also tried under

Table 5 Physiochemical properties and medicinal chemistry data of compound **16h** calculated using ADMETlab 3.0 software[a]

	Compound **16h**	Recommended limit
Physicochemical property		
log *P*	6.475	0 to 3 log octanol/water
log *S*	−7.094	−4 to 0.5 mol l^{-1}
log *D*	5.292	1 to 3
*n*HA	3.0	0 to 12
*n*HD	0.0	0 to 7
TPSA	26.53	0 to 140 Å^2
nRot	2.0	0 to 11
*n*Ring	5.0	0 to 6
MaxRing	10.0	0 to 18
*n*Rig	27.0	0 to 30
nHet	4.0	1 to 15
fChar	0.0	−4 to 4
%ABS	99.84%	
Medicinal chemistry		
MCE-18	59.871	MCE-18 ≥ 45
NP score	−0.45	−5 to 5
Lipinski rule	Accepted	MW ≤ 500, log *P* ≤ 5, *n*HA ≤ 10, *n*HD ≤ 5, TPSA ≤ 140 Å^2
Pfizer rule	Rejected	log *P* ≤ 3, TPSA ≥ 75 Å^2
Golden triangle	Rejected	200 ≤ MW ≤ 500, −2 ≤ log *D* ≤ 5

[a] Abbreviations: *n*HA: number of hydrogen-bond acceptors, *n*HD: number of hydrogen-bond donors, TPSA: topological polar surface area (in Å^2), *n*Rig: number of rigid bonds, *n*Ring: number of rings, MaxRing: number of atoms in the biggest ring, %ABS: percentage absorption.

Table 6 ADMET properties of the most potent compound **16h** calculated using ADMETlab 3.0 software[a]

ADMET	Compound **16h**	Recommended limit
Absorption		
Caco-2 permeability	−4.578	≥−5.15 log unit
MDCK permeability	−4.56	≤20 × 10^{-6} cm s^{-1}
Pgp-inhibitor	0.998	0 to 0.5
Pgp-substrate	0.008	0 to 0.5
HIA	0.0	
$F_{50\%}$	0.004	
Distribution		
PPB	99.266%	≤90%
BBB	0.999	<0.5
VD	0.377	0.04 to 20 l kg^{-1}
Fu	0.409%	5% to 20%
Metabolism		
CYP1A2 inhibitor	1.0	0 to 0.5
CYP1A2 substrate	0.997	0 to 0.5
CYP2C19 inhibitor	1.0	0 to 0.5
CYP2C19 substrate	0.986	0 to 0.5
CYP2C9 inhibitor	1.0	0 to 0.5
CYP2C9 substrate	0.922	0 to 0.5
CYP2D6 inhibitor	0.03	0 to 0.5
CYP2D6 substrate	0.047	0 to 0.5
CYP3A4 inhibitor	0.723	0 to 0.5
CYP3A4 substrate	0.996	0 to 0.5
Excretion		
CL	4.967	5 to 15 mL min^{-1} kg^{-1}
$T_{1/2}$	0.541	>4 h
Toxicity		
DILI	0.907	<0.5
Skin sensitization	0.682	<0.5
Eye corrosion	0.0	<1
Eye irritation	0.277	<1

[a] MDCK: apparent permeability in Madin–Darby canine kidney cells, HIA: human intestinal absorption, VD: volume of distribution, $F_{50\%}$: 50% bioavailability, PPB: plasma protein binding, BBB: blood–brain barrier, PGP: plasma glycoprotein, CL: clearance, DILI: drug-induced liver injury, $T_{1/2}$: half-life period.

microwave conditions (100 W, 120 °C, 20–30 min), providing very good yields of the products **16(a–u)** in comparison to the conventional heating method (Schemes 3 and 4).

4.1.5. 3-(2,2-Dimethyl-2*H*-chromen-4-yl)-2-phenylimidazo-[1,2-*a*]pyridine (16a). White solid (0.176 g, 88% yield): m.p. = 265–267 °C, ^{1}H NMR (400 MHz, $CDCl_3$): δ (ppm) 7.90–7.87 (m, 2H, ArH), 7.70–7.65 (m, 2H, ArH), 7.37–7.33 (m, 2H, ArH), 7.29–7.27 (m, 1H, ArH), 7.21–7.17 (m, 2H, ArH), 6.95 (dd, J_1 = 8.4 Hz, J_2 = 1.2 Hz, 1H, ArH), 6.77–6.69 (m, 2H, ArH), 6.61 (dd, J_1 = 8.0 Hz, J_2 = 2 Hz, 1H, ArH), 5.80 (s, 1H), 1.55 (s, 3H), 1.48 (s, 3H), ^{13}C NMR (100 MHz, $CDCl_3$): δ (ppm) 153.3, 145.0, 143.8, 135.3, 133.8, 130.2, 128.3 (2C), 127.8 (2C), 127.6, 124.7, 124.5, 124.3, 123.7, 121.3, 119.9, 117.4, 117.2, 116.7, 112.2, 76.1, 28.2, 25.6, HRMS (ESI) calculated for $C_{24}H_{20}N_2O$ $[M + H]^+$: 353.1654, found 353.1616.

4.1.6. 3-(2,2-Dimethyl-2*H*-chromen-4-yl)-7-methyl-2-phenylimidazo-[1,2-*a*]pyridine (16b). Pure white solid (0.182 g, 91% yield): m.p. = 230–235 °C, ^{1}H NMR (400 MHz, $CDCl_3$): δ (ppm) 7.87 (d, J = 7.6 Hz, 2H, ArH), 7.52 (d, J = 6.8 Hz, 1H, ArH), 7.44 (s, 1H, ArH), 7.35–7.31 (m, 2H, ArH), 7.28–7.24 (m, 1H, ArH), 7.21–7.16 (m, 1H, ArH), 6.94 (d, J = 8.4 Hz, 1H, ArH), 6.74 (m, 1H, ArH), 6.62 (d, J = 7.2 Hz, 1H, ArH), 6.53 (dd, J_1 = 6.8 Hz, J_2 = 1.6 Hz, 1H, ArH), 5.77 (s, 1H), 2.40 (s, 3H), 1.54 (s, 3H), 1.47 (s, 3H), ^{13}C NMR (100 MHz, $CDCl_3$): δ (ppm) 153.3, 145.4, 143.5, 135.8, 135.1, 133.9, 130.1, 128.2 (2C), 127.7 (2C), 127.5, 124.6, 123.7, 123.5, 121.3, 120.1, 117.1, 116.1, 115.7, 114.8, 76.1, 28.2, 25.5, 21.3, HRMS (ESI) calculated for $C_{25}H_{22}N_2O$ $[M + H]^+$: 367.1810, found 367.1781.

4.1.7. 3-(2,2-Dimethyl-2*H*-chromen-4-yl)-6-methyl-2-phenylimidazo-[1,2-*a*]pyridine (16c). Pure white solid (0.180 g, 90% yield): m.p. = 224–228 °C, ^{1}H NMR (400 MHz, $CDCl_3$): δ (ppm) 7.89–7.86 (m, 2H, ArH), 7.58 (d, J = 9.2 Hz, 1H, ArH), 7.42 (s, 1H, ArH), 7.35–7.27 (m, 3H, ArH), 7.20–7.18 (m, 1H, ArH), 7.05 (dd, J_1 = 9.2 Hz, J_2 = 2 Hz, 1H, ArH), 6.96 (dd, J_1 = 8.4 Hz, J_2 = 1.2 Hz, 1H, ArH), 6.77–6.73 (m, 1H, ArH), 6.62 (dd, J_1 = 7.6 Hz, J_2 = 1.6 Hz, 1H, ArH), 5.78 (s, 1H), 2.23 (s, 3H), 1.57 (s, 3H), 1.48 (s, 3H), ^{13}C NMR (100 MHz, $CDCl_3$): δ (ppm) 153.2, 144.1, 143.6, 135.2, 134.1, 130.2, 128.2 (2C), 127.9, 127.7 (2C), 127.5, 124.6, 123.8, 121.9, 121.8, 121.4, 120.1, 117.2, 116.7, 116.5, 76.2, 28.2, 25.6, 18.2, HRMS (ESI) calculated for $C_{25}H_{22}N_2O$ $[M + H]^+$: 367.1810, found 367.1790.

4.1.8. 2-(4-Chlorophenyl)-3-(2,2-dimethyl-2*H*-chromen-4-yl)-imidazo[1,2-*a*]pyridine (16d). Pale yellow solid (0.184 g, 92% yield): m.p. = 256–258 °C, ^{1}H NMR (400 MHz, $CDCl_3$): δ (ppm) 7.84–7.83 (m, 2H, ArH), 7.78 (d, J = 16.0 Hz, 1H, ArH), 7.68 (d, J = 8.0 Hz, 1H, ArH), 7.33–7.26 (m, 3H, ArH), 7.23–7.19 (m, 1H, ArH), 6.97–6.95 (dd, J_1 = 7.6 Hz, J_2 = 0.8 Hz, 1H, ArH), 6.79–6.73 (m, 2H, ArH), 6.58 (dd, J_1 = 7.2 Hz, J_2 = 1.2 Hz, 1H, ArH), 5.80 (s, 1H), 1.56 (s, 3H), 1.48 (s, 3H), ^{13}C NMR (100 MHz, $CDCl_3$): δ (ppm) 153.3, 144.6, 141.9, 135.6, 133.8, 131.6, 130.4, 129.0

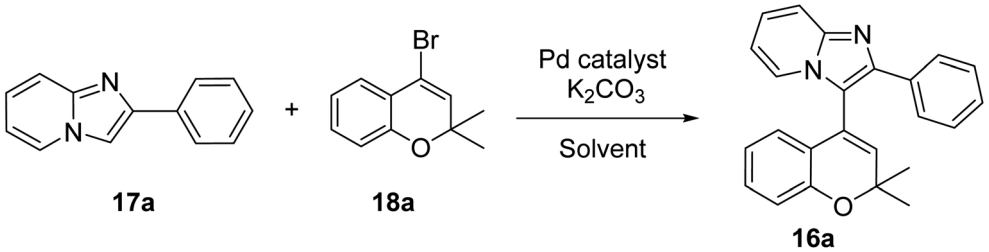

Scheme 3 Screening of reaction conditions for the coupling of **17a** and **18a**.

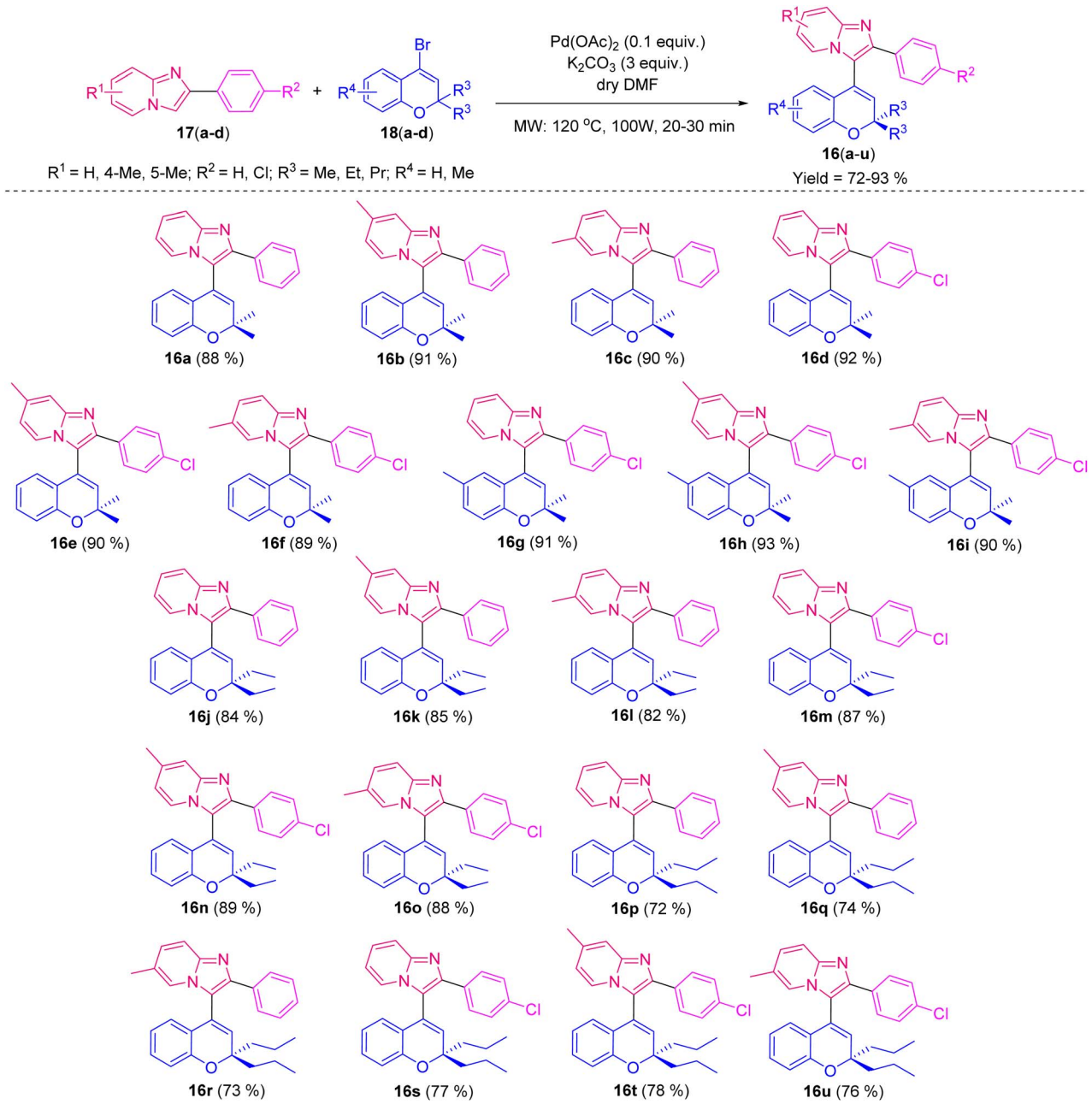

Scheme 4 Synthesis of a library of 3-(2,2-dialkyl-2*H*-chromen-4-yl)-2-phenylimidazo[1,2-*a*]pyridine derivatives **16(a–u)**.

(2C), 128.6 (2C), 125.6, 124.3 (2C), 123.3, 121.4, 119.6, 117.3, 117.1, 116.8, 112.8, 76.1, 28.1, 25.6, HRMS (ESI) calculated for $C_{24}H_{19}ClN_2O$ $[M + H]^+$: 387.1264, found 387.1292 and $[M + H + 2]^+$ 389.1254.

4.1.9. 2-(4-Chlorophenyl)-3-(2,2-dimethyl-2*H*-chromen-4-yl)-7-methylimidazo-[1,2-*a*]pyridine (16e). Cream white solid (0.181 g, 90% yield): m.p. = 260–262 °C, ^{1}H NMR (400 MHz, $CDCl_3$): δ (ppm) 7.82 (d, J = 8.0 Hz, 2H, ArH), 7.56–7.52 (m, 2H, ArH), 7.31 (d, J = 8.0 Hz, 2H, ArH), 7.22–7.18 (m, 1H, ArH), 6.95 (dd, J_1 = 9.2 Hz, J_2 = 0.8 Hz 1H, ArH), 6.77–6.73 (m, 1H, ArH), 6.61–6.57 (m, 2H, ArH), 5.78 (s, 1H), 2.42 (s, 3H), 1.56 (s, 3H), 1.48 (s, 3H), ^{13}C NMR (100 MHz, $CDCl_3$): δ (ppm) 153.3, 144.9, 141.3, 137.1, 135.5, 133.7, 131.5, 130.4, 129.0 (2C), 128.5 (2C), 124.4, 123.6, 123.2, 121.4, 119.7, 117.3, 116.3, 115.6, 115.4, 76.1, 28.1, 25.6, 21.3. HRMS (ESI) calculated for $C_{25}H_{21}ClN_2O$ $[M + H]^+$: 401.1420, found 401.1390 and $[M + H + 2]^+$ 403.1374.

4.1.10. 2-(4-Chlorophenyl)-3-(2,2-dimethyl-2*H*-chromen-4-yl)-6-methylimidazo-[1,2-*a*]pyridine (16f). Chrome yellow-colored solid (0.178 g, 89% yield); m.p. = 250–252 °C.^{1}H NMR (400 MHz, $CDCl_3$): δ (ppm) 7.80 (d, J = 8.8 Hz, 2H, ArH), 7.57 (d, J = 9.2 Hz, 1H, ArH), 7.42 (s, 1H, ArH), 7.30 (d, J = 8.4 Hz, 2H, ArH), 7.23–7.19 (m, 1H, ArH), 7.08–7.05 (m, 1H, ArH), 6.96 (d, J = 7.6 Hz, 1H, ArH), 6.78–6.74 (m, 1H, ArH), 6.60–6.59 (m, 1H, ArH), 5.77 (s, 1H), 2.23 (s, 3H), 1.58 (s, 3H), 1.49 (s, 3H), ^{13}C NMR

(100 MHz, $CDCl_3$): δ (ppm) 153.2, 144.1, 142.4, 135.3, 133.3, 132.5, 130.3, 128.8 (2C), 128.4 (2C), 128.2, 124.5, 123.7, 122.1, 121.8, 121.4, 119.9, 117.2, 116.7, 116.5, 76.1, 28.1, 25.6, 18.2. HRMS (ESI) calculated for $C_{25}H_{21}ClN_2O$ $[M + H]^+$: 401.1420, found 401.1419 and $[M + H + 2]^+$ 403.1402.

4.1.11 2-(4-Chlorophenyl)-3-(2,2,6-trimethyl-2*H*-chromen-4-yl)-imidazo-[1,2-*a*]pyridine (16g). Sunshine white solid (0.182 g, 91% yield): m.p. = 254–258 °C, ^{1}H NMR (400 MHz, $CDCl_3$): δ (ppm) 7.83–7.81 (m, 2H, ArH), 7.69–7.64 (m, 2H, ArH), 7.32–7.30 (m, 2H, ArH), 7.24–7.20 (m, 1H, ArH), 7.00 (dd, J_1 = 8.4 Hz, J_2 = 2 Hz, 1H, ArH), 6.85 (d, J = 8.4 Hz, 1H, ArH), 6.74–6.70 (m, 1H, ArH), 6.38 (d, J = 2 Hz, 1H, ArH), 5.76 (s, 1H), 2.06 (s, 3H), 1.54 (s, 3H), 1.46 (s, 3H), ^{13}C NMR (100 MHz, $CDCl_3$): δ (ppm) 151.0, 145.0, 142.5, 135.5, 133.5, 132.3, 130.8, 130.7, 129.0 (2C), 128.5 (2C), 125.0, 124.6, 124.3, 123.6, 119.5, 117.4, 117.1, 117.0, 112.4, 75.8, 28.0, 25.4, 20.5, HRMS (ESI) calculated for $C_{25}H_{21}ClN_2O$ $[M + H]^+$: 401.1510, found 401.1391 and $[M + H + 2]^+$ 403.1396.

4.1.12. 2-(4-Chlorophenyl)-7-methyl-3-(2,2,6-trimethyl-2*H*-chromen-4-yl)-imidazo-[1,2-*a*]pyridine (16h). Faded greenish white solid (0.186 g, 93% yield): m.p. = 250–254 °C, ^{1}H NMR (400 MHz, $CDCl_3$): δ (ppm) 7.82–7.80 (m, 2H, ArH), 7.53 (d, J = 7.2 Hz, 1H, ArH), 7.43 (s, 1H), 7.32–7.29 (m, 2H, ArH), 7.00 (dd, J_1 = 8.4 Hz, J_2 = 2 Hz, 1H, ArH), 6.85 (d, J = 8.4 Hz, 1H, ArH), 6.55 (dd, J_1 = 6.8 Hz, J_2 = 1.2 Hz, 1H, ArH), 6.39 (d, J = 2 Hz, 1H, ArH), 5.75 (s, 1H), 2.41 (s, 3H), 2.07 (s, 3H), 1.54 (s, 3H), 1.46 (s, 3H), ^{13}C NMR (100 MHz, $CDCl_3$): δ (ppm) 151.0, 145.5, 142.3, 136.1, 135.4, 133.3, 132.5, 130.7, 130.7, 128.9 (2C), 128.4 (2C), 124.7, 123.7, 123.5, 119.6, 117.0, 116.4, 115.7, 115.0, 75.8, 28.0, 25.3, 21.3, 20.5, HRMS (ESI) calculated for $C_{26}H_{23}ClN_2O$ $[M + H]^+$: 415.1577, found 415.1551 and $[M + H + 2]^+$ 417.1532.

4.1.13. 2-(4-Chlorophenyl)-6-methyl-3-(2,2,6-trimethyl-2*H*-chromen-4-yl)-imidazo-[1,2-*a*]pyridine (16i). White solid (0.180 g, 90% yield): m.p. = 224–228 °C, ^{1}H NMR (400 MHz, $CDCl_3$): δ (ppm) 7.81 (d, J = 8.4 Hz, 2H, ArH), 7.58 (d, J = 9.2 Hz, 1H, ArH), 7.42 (s, 1H, ArH), 7.30 (d, J = 8.8 Hz, 2H, ArH), 7.09–7.00 (m, 2H, ArH), 6.86 (d, J = 8.0 Hz, 1H, ArH), 6.39 (d, J = 2.0 Hz, 1H, ArH), 5.75 (s, 1H), 2.24 (s, 3H), 2.07 (s, 3H), 1.56 (s, 3H), 1.46 (s, 3H), ^{13}C NMR (100 MHz, $CDCl_3$): δ (ppm) 150.9, 144.1, 142.2, 135.5, 133.3, 132.5, 130.8, 128.8 (3C), 128.4 (3C), 128.2, 124.7, 123.8, 122.1, 121.7, 119.7, 117.0, 116.6, 75.9, 28.0, 25.4, 20.5, 18.2, HRMS (ESI) calculated for $C_{26}H_{23}ClN_2O$ $[M + H]^+$: 415.1577, found 415.1556 and $[M + H + 2]^+$ 417.1552.

4.1.14. 3-(2, 2-Diethyl-2*H*-chromen-4-yl)-2-phenylimidazo-[1,2-*a*]pyridine (16j). White solid (0.168 g, 84% yield): m.p. = 182–185 °C, ^{1}H NMR (400 MHz, $CDCl_3$): δ (ppm) 7.85–7.82 (m, 2H, ArH), 7.67–7.63 (m, 2H, ArH), 7.29–7.25 (m, 2H, ArH), 7.21–7.18 (m, 1H, ArH), 7.16–7.07 (m, 2H, ArH), 6.86 (dd, J_1 = 8.4 Hz, J_2 = 0.8 Hz, 1H, ArH), 6.69–6.60 (m, 2H, ArH), 6.49 (dd, J_1 = 7.2 Hz, J_1 = 1.2 Hz, 1H, ArH), 5.66 (s, 1H), 1.85–1.58 (m, 4H), 0.96 (t, J = 7.2 Hz, 3H), 0.85 (t, J = 7.6 Hz, 3H), ^{13}C NMR (100 MHz, $CDCl_3$): δ (ppm) 154.0, 144.7, 143.1, 133.9, 133.4, 130.2, 128.3 (2C), 127.8 (3C), 125.0, 124.9, 124.5, 124.1, 120.9, 119.6, 117.2, 117.0, 116.7, 112.5, 81.7, 31.5, 31.2, 8.3, 7.7, HRMS (ESI) calculated for $C_{26}H_{24}N_2O$ $[M + H]^+$: 381.1967, found 381.1936.

4.1.15. 3-(2,2-Diethyl-2*H*-chromen-4-yl)-7-methyl-2-phenyl-imidazo-[1,2-*a*]pyridine (16k). White solid (0.171 g, 85% yield): m.p. = 210–212 °C, ^{1}H NMR (400 MHz, $CDCl_3$): δ (ppm) 7.83–7.81 (m, 2H, ArH), 7.50 (d, J = 7.2 Hz, 1H, ArH), 7.41 (s, 1H, ArH), 7.27–7.24 (m, 2H, ArH), 7.20–7.16 (m, 1H, ArH), 7.11–7.07 (m, 1H, ArH), 6.85 (dd, J_1 = 8.4 Hz, J_2 = 1.2 Hz, 1H, ArH), 6.64–6.60 (m, 1H, ArH), 6.50 (dd, J_1 = 7.2 Hz, J_2 = 1.2 Hz, 2H, ArH), 5.64 (s, 1H), 2.34 (s, 3H), 1.84–1.57 (m, 4H), 0.95 (t, J = 7.2 Hz, 3H), 0.84 (t, J = 7.2 Hz, 3H), ^{13}C NMR (100 MHz, $CDCl_3$): δ (ppm) 154.1, 145.2, 142.9, 136.2, 133.9, 133.6, 130.2, 128.4 (2C), 127.8 (2C), 127.7, 125.1, 124.7, 123.5, 120.9, 119.9, 116.7, 116.5, 115.7, 115.3, 81.8, 31.6, 31.3, 21.4, 8.4, 7.8, HRMS (ESI) calculated for $C_{27}H_{26}N_2O$ $[M + H]^+$: 395.2123, found 395.2091.

4.1.16. 3-(2,2-Diethyl-2*H*-chromen-4-yl)-6-methyl-2-phenyl-imidazo-[1,2-*a*]pyridine (16l). White solid (0.165 g, 82% yield): m.p. = 158–162 °C, ^{1}H NMR (400 MHz, $CDCl_3$): δ (ppm) 7.82–7.80 (m, 2H, ArH), 7.54 (d, J = 9.2 Hz, 1H, ArH), 7.40 (s, 1H, ArH), 7.27–7.23 (m, 2H, ArH), 7.20–7.18 (m, 1H, ArH) 7.12–7.08 (m, 1H, ArH), 7.00 (dd, J_1 = 9.2 Hz, J_2 = 2.0 Hz, 1H, ArH), 6.86 (d, J = 8.4 Hz, 1H, ArH), 6.65–6.61 (m, 1H, ArH), 6.50 (dd, J_1 = 8.0 Hz, J_2 = 1.6 Hz, 1H, ArH), 5.64 (s, 1H), 2.16 (s, 3H), 1.85–1.60 (m, 4H), 0.97 (t, J = 7.2 Hz, 3H), 0.85 (t, J = 7.2 Hz, 3H), ^{13}C NMR (100 MHz, $CDCl_3$): δ (ppm) 154.0, 143.8, 143.0, 133.8, 133.6, 130.1, 128.3 (2C), 128.1, 127.6 (2C), 127.6, 125.1, 124.6, 122.2, 121.6, 120.9, 119.8, 116.6 (2C), 81.7, 31.5, 31.1, 18.3, 8.2, 7.7, HRMS (ESI) calculated for $C_{27}H_{26}N_2O$ $[M + H]^+$: 395.2123, found 395.2101.

4.1.17. 2-(4-Chlorophenyl)-3-(2,2-diethyl-2*H*-chromen-4-yl)-imidazo[1,2-*a*]pyridine (16m). Cream white solid (0.174 g, 87% yield): m.p. = 212–215 °C, ^{1}H NMR (400 MHz, $CDCl_3$): δ (ppm) 7.81–7.77 (m, 2H, ArH), 7.71 (d, J = 8.8 Hz, 1H, ArH), 7.67–7.65 (m, 1H, ArH), 7.27–7.24 (m, 2H, ArH), 7.22 (d, J = 8.4 Hz, 1H, ArH), 7.14–7.10 (m, 1H, ArH), 6.87 (dd, J_1 = 8.0 Hz, J_2 = 0.8 Hz, 1H, ArH), 6.75–6.72 (m, 1H, ArH), 6.66–6.62 (m, 1H, ArH), 6.46 (dd, J_1 = 8.0 Hz, J_2 = 2 Hz, 1H, ArH), 5.68 (s, 1H), 1.87–1.60 (m, 4H), 0.96 (t, J = 7.2 Hz, 3H), 0.87 (t, J = 7.6 Hz, 3H), ^{13}C NMR (100 MHz, $CDCl_3$): δ (ppm) 154.0, 144.7, 141.8, 134.1, 133.7, 131.8, 130.4, 128.9 (2C), 128.6 (2C), 125.4, 124.7, 124.4, 124.1, 120.9, 119.4, 117.2, 117.1, 116.8, 112.8, 81.7, 31.5, 31.1, 8.3, 7.8, HRMS (ESI) calculated for $C_{26}H_{23}ClN_2O$ $[M + H]^+$: 415.1577, found 415.1580 and $[M + H + 2]^+$ 417.1560.

4.1.18. 2-(4-Chlorophenyl)-3-(2,2-diethyl-2*H*-chromen-4-yl)-7-methylimidazo[1,2-*a*]pyridine (16n). Sunshine white solid (0.178 g, 89% yield): m.p. = 232–235 °C, ^{1}H NMR (400 MHz, $CDCl_3$): δ (ppm) 7.84–7.80 (m, 2H, ArH), 7.57 (d, J = 7.2 Hz, 1H, ArH), 7.42 (s, 1H), 7.30–7.28 (m, 2H, ArH), 7.19–7.15 (m, 1H, ArH), 6.93 (dd, J_1 = 8.4 Hz, J_2 = 1.2 Hz, 1H, ArH), 6.71–6.67 (m, 1H, ArH), 6.57–6.54 (m, 2H, ArH), 5.71 (s, 1H), 2.41 (s, 3H), 1.92–1.66 (m, 4H), 1.02 (t, J = 7.2 Hz 3H), 0.94 (t, J = 7.6 Hz, 3H), ^{13}C NMR (100 MHz, $CDCl_3$): δ (ppm) 154.0, 145.5, 142.0, 136.0, 133.8, 133.3, 132.5, 130.2, 128.8 (2C), 128.4 (2C), 124.9, 124.5, 123.3, 120.9, 119.6, 116.7, 116.5, 115.7, 115.1, 81.6, 31.4, 31.1, 21.3, 8.3, 7.8, HRMS (ESI) calculated for $C_{27}H_{25}ClN_2O$ $[M + H]^+$: 429.1733, found 429.1704 and $[M + H + 2]^+$ 431.1700.

4.1.19. 2-(4-Chlorophenyl)-3-(2,2-diethyl-2*H*-chromen-4-yl)-6-methylimidazo[1,2-*a*]pyridine (16o). Light cream white solid (0.176 g, 88% yield): m.p. = 208–212 °C, ^{1}H NMR (400 MHz, $CDCl_3$): δ (ppm) 7.82 (d, J = 8.0 Hz, 2H, ArH), 7.57 (d, J = 9.2 Hz, 1H, ArH), 7.47 (s, 1H), 7.29 (d, J = 8.4 Hz, 2H, ArH), 7.20–7.16

(m, 1H, ArH), 7.07 (d, J = 9.2 Hz, 1H, ArH), 6.94 (d, J = 8.4 Hz, 1H, ArH), 6.72–6.68 (m, 1H, ArH), 6.56–6.54 (m, 1H, ArH), 5.72 (s, 1H), 2.24 (s, 3H), 1.92–1.71 (m, 4H), 1.05 (t, J = 7.4 Hz, 3H), 0.94 (t, J = 7.2 Hz, 3H), ^{13}C NMR (100 MHz, $CDCl_3$): δ (ppm) 153.9, 144.1, 142.1, 133.9, 133.3, 132.5, 130.2, 128.8 (2C), 128.4 (2C), 128.1, 125.0, 124.5, 122.2, 121.6, 120.9, 119.7, 116.7 (2C), 81.6, 31.5, 31.1, 30.9, 18.3, 8.3, 7.8, HRMS (ESI) Calculated for $C_{27}H_{25}ClN_2O$ $[M + H]^+$: 429.1733, found 429.1735 and $[M + H + 2]^+$ 431.1718.

4.1.20. 3-(2,2-Dipropyl-2*H*-chromen-4-yl)-2-phenylimidazo-[1,2-*a*]pyridine (16p). Dusty white solid (0.143 g, 72% yield): m.p. = 152–154 °C, ^{1}H NMR (400 MHz, $CDCl_3$): δ (ppm) 7.83–7.81 (m, 2H, ArH), 7.65–7.60 (m, 2H, ArH), 7.29–7.25 (m, 2H, ArH), 7.23–7.20 (m, 1H, ArH), 7.17–7.07 (m, 2H, ArH), 6.83 (dd, J_1 = 8.4 Hz, J_2 = 1.2 Hz, 1H, ArH), 6.67–6.61 (m, 2H, ArH), 6.49 (dd, J_1 = 7.6 Hz, J_2 = 1.6 Hz, 1H, ArH), 5.65 (s, 1H), 1.75–1.24 (m, 8H), 0.88–0.79 (m, 6H), ^{13}C NMR (100 MHz, $CDCl_3$): δ (ppm) 153.9, 144.8, 143.4, 134.3, 133.6, 130.1, 128.2 (2C), 127.8 (2C), 127.7, 124.8, 124.5, 124.3, 124.1, 120.8, 119.6, 117.3, 117.0, 116.6, 112.4, 81.3, 41.7, 41.5, 17.4, 16.7, 14.4 (2C), HRMS (ESI) calculated for $C_{28}H_{28}N_2O$ $[M + H]^+$: 409.2280, found 409.2302.

4.1.21. 3-(2,2-Dipropyl-2*H*-chromen-4-yl)-7-methyl-2-phenylimidazo[1,2-*a*]pyridine (16q). Radiant white solid (0.149 g, 74% yield): m.p. = 190–196 °C, ^{1}H NMR (400 MHz, $CDCl_3$): δ (ppm) 7.82–7.79 (m, 2H, ArH), 7.48 (d, J = 6.8 Hz, 1H, ArH), 7.38 (s, 1H. ArH), 7.28–7.26 (m, 2H, ArH), 7.21–7.18 (m, 1H, ArH), 7.10–7.07 (m, 1H, ArH), 6.83 (d, J = 8.0 Hz, 1H, ArH), 6.65–6.61 (m, 1H, ArH), 6.51–6.48 (m, 2H, ArH), 5.63 (s, 1H), 2.34 (s, 3H), 1.75–1.30 (m, 8H), 0.88–0.79 (m, 6H), ^{13}C NMR (100 MHz, $CDCl_3$): δ (ppm) 153.9, 145.3, 143.1, 135.8, 134.1, 133.8, 130.1, 128.2 (2C), 127.7 (2C), 127.5, 124.6, 124.4, 123.4, 120.8, 119.7, 116.5, 116.4, 115.7, 115.0, 81.3, 41.7, 41.5, 21.3, 17.4, 16.7, 14.4 (2C), HRMS (ESI) calculated for $C_{29}H_{30}N_2O$ $[M + H]^+$: 423.2436, found 423.2437.

4.1.22. 3-(2,2-Dipropyl-2*H*-chromen-4-yl)-6-methyl-2-phenylimidazo-[1,2-*a*]pyridine (16r). Radiant white solid (0.146, 73% yield): m.p. = 182–186 °C, ^{1}H NMR (400 MHz, $CDCl_3$): δ (ppm) 7.80 (d, J = 7.2 Hz, 2H, ArH), 7.52 (d, J = 9.2 Hz, 1H, ArH), 7.38 (s, 1H, ArH), 7.27–7.23 (m, 2H, ArH), 7.20–7.17 (m, 1H, ArH), 7.10–7.09 (m, 1H, ArH), 6.99 (dd, J_1 = 9.2 Hz, J_2 = 1.6 Hz, 1H, ArH), 6.83 (dd, J_1 = 8.4 Hz, J_2 = 0.8 Hz, 1H, ArH), 6.63–6.61 (m, 1H, ArH), 6.50 (dd, J_1 = 8.0 Hz, J_2 = 2.0 Hz, 1H, ArH), 5.63 (s, 1H), 2.16 (s, 3H), 1.74–1.27 (m, 8H), 0.89–0.78 (m, 6H), ^{13}C NMR (100 MHz, $CDCl_3$): δ (ppm) 153.9, 143.9, 143.2, 134.1, 133.8, 130.1, 128.2 (2C), 127.9, 127.6 (2C), 127.5, 124.5, 124.6, 122.0, 121.6, 120.8, 119.7, 116.7, 116.6, 116.5, 81.3, 41.7, 41.4, 18.3, 17.4, 16.7, 14.4 (2C), HRMS (ESI) calculated for $C_{29}H_{30}N_2O$ $[M + H]^+$: 423.2436, found 423.2437.

4.1.23. 2-(4-Chlorophenyl)-3-(2, 2-dipropyl-2*H*-chromen-4-yl)-imidazo-[1,2-*a*]pyridine (16s). Grayish white solid (0.154 g, 77% yield): m.p. = 204–208 °C, ^{1}H NMR (400 MHz, $CDCl_3$): δ (ppm) 7.83 (d, J = 8.8 Hz, 2H, ArH), 7.70–7.66 (m, 2H, ArH), 7.32–7.28 (m, 2H, ArH), 7.25–7.15 (m, 2H, ArH) 6.91 (d, J = 9.2 Hz, 1H, ArH), 6.76–6.68 (m, 2H, ArH), 6.53 (dd, J_1 = 7.6 Hz, J_2 = 1.6 Hz 1H, ArH), 5.72 (s, 1H), 1.81–1.58 (m, 8H), 0.96–0.89 (m, 6H), ^{13}C NMR (100 MHz, $CDCl_3$): δ (ppm) 153.9, 145.0, 142.4, 134.4, 133.5, 132.3, 130.3, 129.0 (2C), 128.4 (2C), 124.9, 124.4, 124.3, 124.1, 120.9, 119.4, 117.4, 117.1, 116.7, 112.5, 81.3, 41.6, 41.4, 17.4, 16.8, 14.4 (2C), HRMS (ESI) calculated for $C_{28}H_{27}ClN_2O$ $[M + H]^+$: 443.1890, found 443.1846 and $[M + H + 2]^+$ 445.1844.

4.1.24. 2-(4-Chlorophenyl)-3-(2,2-dipropyl-2*H*-chromen-4-yl)-7-methylimidazo[1,2-*a*]pyridine (16t). Cream white solid (0.156 g, 78% yield): m.p. = 235–240 °C, ^{1}H NMR (400 MHz, $CDCl_3$): δ (ppm) 7.80 (d, J = 8.8 Hz, 2H, ArH), 7.55 (d, J = 7.2 Hz, 1H, ArH), 7.42 (s, 1H), 7.29 (d, J = 8.8 Hz, 2H, ArH), 7.17–7.15 (m, 1H), 6.91–6.89 (dd, J_1 = 8.4 Hz, J_2 = 1.2 Hz, 1H, ArH), 6.69–6.68 (m, 1H), 6.58–6.53 (m, 2H), 5.69 (s, 1H), 2.41 (s, 3H), 1.80–1.36 (m, 8H), 0.98–0.88 (m, 6H), ^{13}C NMR (100 MHz, $CDCl_3$): δ (ppm) 153.9, 145.5, 142.2, 136.0, 134.3, 133.4, 132.5, 130.2, 128.9 (2C), 128.4 (2C), 124.5, 124.3, 123.3, 120.8, 119.5, 116.8, 116.6, 115.7, 115.1, 81.3, 41.8, 41.5, 21.3, 17.4, 16.8, 14.4 (2C), HRMS (ESI) calculated for $C_{29}H_{29}ClN_2O$ $[M + H]^+$: 457.2046, found 457.2017 and $[M + H + 2]^+$ 459.2003.

4.1.25. 2-(4-Chlorophenyl)-3-(2,2-dipropyl-2*H*-chromen-4-yl)-7-6-methylimidazo-[1,2-*a*]pyridine (16u). Chrome white solid (0.152 g, 76% yield): m.p. = 222–225 °C, ^{1}H NMR (400 MHz, $CDCl_3$): δ (ppm) 7.80 (d, J = 8.4 Hz, 2H, ArH), 7.57 (d, J = 9.2 Hz, 1H, ArH), 7.46 (s, 1H, ArH), 7.29 (d, J = 8.8 Hz, 2H, ArH), 7.20–7.16 (m, 1H), 7.07 (dd, J_1 = 9.6 Hz, J_2 = 2 Hz, 1H, ArH), 6.91 (dd, J_1 = 8.4 Hz, J_2 = 1.2 Hz, 1H, ArH), 6.72–6.68 (m, 1H, ArH), 6.54 (dd, J_1 = 7.6 Hz, J_2 = 1.6 Hz, 1H, ArH), 5.70 (s, 1H), 2.24 (s, 3H), 1.86–1.32 (m, 8H), 0.97–0.88 (m, 6H), ^{13}C NMR (100 MHz, $CDCl_3$): δ (ppm) 153.8, 144.1, 142.1, 134.3, 133.3, 132.6, 130.2, 128.8 (2C), 128.4 (2C), 128.1, 124.5, 124.4, 122.2, 121.6, 120.9, 119.6, 116.8, 116.7, 116.7, 81.3, 41.6, 41.3, 18.3, 17.4, 16.8, 14.4 (2C), HRMS (ESI) calculated for $C_{29}H_{29}ClN_2O$ $[M + H]^+$: 457.2046, found 457.2025 and $[M + H + 2]^+$ 459.2008.

4.2 Antibacterial evaluation

Using agar well diffusion procedures, all of the synthesized compounds were tested for their antibacterial sensitivity *in vitro* against the test organisms, namely, the Gram-positive bacteria *S. aureus* and Gram-negative bacteria *E. coli*. Gentamicin was chosen as the standard drug. The synthesised compounds were first dissolved in DMSO. The zone of inhibition (ZI) was then evaluated using Mueller–Hinton agar plates. Initially, a sterilized Petri plate was filled with a 25 mL aliquot of the sterilized media. Once the media solidified, the microbial suspension was dispersed over the agar medium and a sterilized cork borer was used to create a well 6 mm in diameter. Next, for the ZI assessment, 80 μl of the test materials (100 μg mL^{-1}) were placed into each well. Subsequently, the synthesized compounds were diluted at different concentrations (10, 20, 30, 40, 50, 60, 70, 80, and 100 μg mL^{-1}) in order to determine the minimum inhibitory concentration (MIC) by assay. Next, the bacterial inhibitory efficacy was assessed for every fractionated entity in a 96-well plate experiment.[26–28]

4.3 Molecular docking studies

The docking computation of the synthesized compounds **16(a–u)** was performed with AutoDock Tools version 4.2. The protein data bank (**https://www.rcsb.org/**) provided the crystal structures of the bacterial DNA gyrase proteins from *E. coli* and *S. aureus*. ChemDraw Ultra 12.0 was used to create the 3D

structures of the synthesised ligands. During the molecular docking process, polar H-bonds were initially added, while confined ligands containing water molecules were removed, and the other default parameters were used. The docked complex of the ligand–receptor was visualised in two dimensions using PyMOL (**https://www.pymol.org/**) and BIOVIA Discovery Studio R2 2017. The best docking score was then chosen for additional evaluation of its antibacterial activities.[29]

4.4 ADME studies

The ADME and pharmacokinetic properties of all the synthesized compounds were studied on the free online server SwissADME (**https://www.swissadme.ch/**). Initially, chemical structures were drawn on Marvin to generate SMILES, which were then inserted directly on the webpage to initiate the prediction process. The resulting different pharmacokinetic properties and ADME parameters were obtained online and explained.[23,30] The *in silico* ADMET predictions of the potent compound **16h** were carried out using the web-based software ADMETlab 3.0 (**https://admetlab3.scbdd.com/**) using a methodology adopted from Rocha *et al.*[31]

Data availability

The data supporting this article have been included as part of the ESI.†

Author contributions

Rudra Narayan Mishra (RNM): conceptualization, methodology, investigation, formal analysis, data curation, software, writing review & editing; Mohammed Ansar Ahemad (MAA): methodology, formal analysis, data curation. Jasmine Panda (JP): writing original draft, conceptualization, methodology, resources, writing – review & editing. Sabita Nayak (SN): conceptualization, validation, supervision, project administration, funding acquisition, resources, writing – review & editing. Seetaram Mohapatra (SRM): supervision, resources, writing – review & editing, funding acquisition. Chita Ranjan Sahoo (CRS): antibacterial studies, resources, software.

Conflicts of interest

The authors declare that they have no known competing financial interests or personal relationships that could have appeared to influence the work reported in this paper.

Acknowledgements

Author SN is thankful to DST ODISHA (2692/ST, Bhubaneswar, 16-7-2020) and LSRB New Delhi (LSRB/01/15001/M/LSRB-372/BTB/2020). Author RNM is thankful to DST ODISHA (Project no. ST-SCST-MISC-0011-2023) for financial support. Also, the author JP acknowledges INSPIRE Programme Division (Ref. DST/INSPIRE/03/2021/000846, New Delhi) for providing financial support in the form of INSPIRE FELLOWSHIP. Author SRM is thankful to SERB-SURE (Project No. SUR/2022/000257) for financial support in the form of research grant. And also thankful to the Centre of Excellence in Environment and Public Health by Higher Education Department, Government of Odisha (Grant no. 26913/HED/HE-PTC-WB-02-17 OHEPEE).

References

1 K. Allel, L. Day, A. Hamilton, L. Lin, L. Furuya-Kanamori, C. E. Moore, T. Van Boeckel, R. Laxminarayan and L. Yakob, *Lancet Planet. Health*, 2023, **7**, e291–e303.
2 (*a*) J. Baranwal, S. Kushwaha, S. Singh and A. Jyoti, *Curr. Phys. Chem.*, 2023, **13**, 2–19; (*b*) J. Panda, B. P. Raiguru, S. Nayak, S. Mohapatra, S. Mohapatra, S. Rout, P. Mohanty, H. S. Biswal, D. Bhattacharya and C. R. Sahoo, *New J. Chem.*, 2024, **48**, 13609–13630; (*c*) B. Samanta, B. S. Panda, S. Mohapatra, S. Nayak, D. Bhattacharya and C. R. Sahoo, *New J. Chem.*, 2024, **48**, 4953–4959.
3 (*a*) S. Renard, A. Olivier, P. Granger, P. Avenet, D. Graham, M. Sevrin, P. George and F. Besnard, *J. Biol. Chem.*, 1999, **274**, 13370–13374; (*b*) M. Mishra, N. P. Mishra, B. P. Raiguru, T. Das, S. Mohapatra, S. Nayak, D. R. Mishra, J. Panda and D. K. Sahoo, *ChemistrySelect*, 2021, **6**, 3570–3575.
4 (*a*) J. Panda, B. P. Raiguru, M. Mishra, S. Mohapatra and S. Nayak, *ChemistrySelect*, 2022, **7**, e202103987; (*b*) N. P. Mishra, S. Mohapatra, T. Das and S. Nayak, *J. Heterocycl. Chem.*, 2022, **59**, 2051–2075.
5 (*a*) H. Depoortere, B. Zivkovic, K. G. Lloyd, D. J. Sanger, G. Perrault, S. Z. Langer and G. Bartholini, *J. Pharmacol. Exp. Ther.*, 1986, **237**, 649–658; (*b*) S. S. Acharya, R. K. Sahoo, P. Mohanty, P. Panda and B. B. Parida, *Chem. Pap.*, 2024, **78**, 8107–8126; (*c*) S. S. Acharya, P. Bhaumick, R. Kumar and L. H. Choudhury, *ACS Omega*, 2022, **7**, 18660–18670.
6 N. Devi, A. K. Jana and V. Singh, *Karbala Int. J. Mod. Sci.*, 2018, **4**, 164–170.
7 A. Kamal, J. S. Reddy, M. J. Ramaiah, D. Dastagiri, E. V. Bharathi, M. V. P. Sagar, S. Pushpavalli, P. Ray and M. Pal-Bhadra, *MedChemComm*, 2010, **1**, 355–360.
8 A. Deep, R. K. Bhatia, R. Kaur, S. Kumar, U. Kumar Jain, H. Singh, S. Batra, D. Kaushik and P. K. Deb, *Curr. Top. Med. Chem.*, 2017, **17**, 238–250.
9 S. Azimi, A. Zonouzi, O. Firuzi, A. Iraji, M. Saeedi, M. Mahdavi and N. Edraki, *Eur. J. Med. Chem.*, 2017, **138**, 729–737.
10 H. C. Kwong, C. C. Kumar, S. H. Mah, Y. L. Mah, T. S. Chia, C. K. Quah, G. K. Lim and S. Chandraju, *Sci. Rep.*, 2019, **9**, 926.
11 B. K. R. Sanapalli, A. Ashames, D. K. Sigalapalli, A. B. Shaik, R. R. Bhandare and V. Yele, *Antibiotics*, 2022, **11**, 1680, DOI: **10.3390/antibiotics11121680**.
12 T. H. Al-Tel, R. A. Al-Qawasmeh and R. Zaarour, *Eur. J. Med. Chem.*, 2011, **46**, 1874–1881.
13 I. Althagafi and E. Abdel-Latif, *Polycyclic Aromat. Compd.*, 2021, **42**, 4487–4500.
14 O. Ebenezer, P. Awolade, N. Koorbanally and P. Singh, *Chem. Biol. Drug Des.*, 2020, **95**, 162–173.

15 S. Kuthyala, M. K. Shankar and G. K. Nagaraja, *ChemistrySelect*, 2018, **3**, 12894–12899.
16 A. Thakur, G. Pereira, C. Patel, V. Chauhan, R. K. Dhaked and A. Sharma, *J. Mol. Struct.*, 2020, **1206**, 1–13.
17 N. P. Mishra, S. Mohapatra, C. R. Sahoo, B. P. Raiguru, S. Nayak, S. Jena and R. N. Padhy, *J. Mol. Struct.*, 2021, **1246**, 1–15.
18 B. P. Raiguru, J. Panda, S. Mohapatra and S. Nayak, *J. Mol. Struct.*, 2023, **1294**, 136282.
19 B. P. Raiguru, S. Mohapatra, S. Nayak, D. Sahal, M. Yadav and B. N. Acharya, *Eur. J. Med. Chem. Rep.*, 2022, **4**, 100029.
20 J. Panda, B. Brahma, S. Nayak, S. Mohapatra, B. P. Raiguru, S. P. Parida and K. Naithani, *J. Heterocycl. Chem.*, 2025, **62**, 99–121.
21 S. P. Parida, S. Mohapatra, S. Nayak, S. Mohapatra, J. Panda and C. R. Sahoo, *ChemistrySelect*, 2024, **9**, e202402223.
22 CCDC 2347891 (16e) contain the ESI† crystallographic data for this paper.
23 (*a*) A. Daina, O. Michielin and V. Zoete, *Sci. Rep.*, 2017, **7**, 42717; (*b*) O. Trott and A. J. Olson, *J. Comput. Chem.*, 2010, **31**, 455–461; (*c*) C. A. Lipinski, F. Lombardo, B. W. Dominy and P. J. Feeney, *Adv. Drug Delivery Rev.*, 2012, **64**, 4–17; (*d*) H. M. Faidallah and S. A. F. Rostom, *Arch. Pharm.*, 2017, **350**, 1–17.
24 S. Rai, F. Ghous, S. Shukla, P. Sharma, P. Trivedi and A. Bishnoi, *J. Mol. Struct.*, 2023, **1292**, 136116.
25 M. R. Xavier, M. M. Marinho, M. S. S. Juliao, E. S. Marinho, F. W. Q. Almeida-Neto, K. K. A. deCastro, J. P. D. Hora, M. N. D. Rocha, A. C. H. Barreto, G. D. Saraiva, P. N. Bandeira, H. S. Santos, H. D. M. Coutinho and A. M. R. Teixeira, *J. Mol. Struct.*, 2024, **1309**, 138019.
26 C. R. Sahoo, S. Maharana, C. P. Mandhata, A. K. Bishoyi, S. K. Paidesetty and R. N. Padhy, *Saudi J. Biol. Sci.*, 2020, **27**, 1580–1586.
27 J. T. Poolman and A. S. Anderson, *Expert Rev. Vaccines*, 2018, **17**, 607–618.
28 I. Wiegand, K. Hilpert and R. E. W. Hancock, *Nat. Protoc.*, 2008, **3**, 163–175.
29 C. R. Sahoo, S. K. Paidesetty, B. Dehury and R. N. Padhy, *J. Biomol. Struct. Dyn.*, 2020, **38**, 5419–5428.
30 A. Daina, O. Michielin and V. Zoete, *J. Chem. Inf. Model.*, 2014, **54**, 3284–3301.
31 M. N. D. Rocha, D. R. Alves, M. M. Marinho, S. M. D. Morais, E. S. Marinho and J. Comput, *Biophys. Chem.*, 2021, **20**, 283–304.